

Table 2 Clinical features of neonatal alveolar rhabdomyosarcoma (non-BWS cases)

No.	Author (Year)	Age at Presentation (Sex)	Primary Tumor	Metastasis			PAX3-FKHR or PAX7-FKHR	Treatment	Outcome
				Skin	Brain	Other			
1	Romos-Perea (1983) [17]	B (F)	Orbit	Multiple	No	No	ND	No	DOD (10 d)
2	Campbell (1987) [18]	B (F)	Foot	No	No	No	ND	Surg, Cx, Rx	DOD (12 mo)
3		5d (F)	Ulnar area	No	No	No	ND	Surg, Rx	DOD (3 mo)
4		14d (M)	Neck	No	No	No	ND	Surg	DOD (1 mo)
5	Kitagawa (1989) [13]	B (F)	?	Multiple	Yes	No	ND	Cx	AWD (14 mo)
6	Schmidt (1993) [19]	B (M)	Retroperitoneum	Multiple	No	No	ND	?	DOD (7 mo)
7	Ito (1997)	14d (F)	Forearm	Multiple	Yes	Orbit, Lung	ND	Surg, Cx	DOD (24 mo)
8	Godambe (2000) [14]	B (F)	Retroperitoneum	Multiple	No	No	Negative	Cx	DOD (1 mo)
9	Grundy (2001) [12]	B (F)	Groin	Multiple	No	No	Negative	Biopsy, Cx	DOD (1 mo)
10		B (M)	Chest wall	Multiple	No	No	Negative	Cx, Rx	DOD (3 mo)
11		B (M)	Thigh	Multiple	Yes	No	Negative	Cx, Surg, SCT	DOD (28 mo)
12		B (F)	Thigh	Multiple	No	No	ND	Cx, Rx	DOD (3 mo)
13	Rodriguez-Galindo (2001) [15]	3w (M)	Prescapular	No	No	No	ND	Cx	NED (22 y)
14		2w (F)	Thigh	Multiple	Yes	LN	ND	Cx	DOD (7 w)
15		4w (F)	Foot	Multiple	Yes	LN	Positive	Cx	DOD (12 mo)
16	Chigurupati (2002)	B (F)	Nasal	No	No	No	Positive	Surg, Cx	DOD (30 mo)
17	Brecher (2003) [16]	2w (M)	Lip	No	No	No	Positive	Cx	NED (6 mo)
18	Shah (2004)	3w (M)	Prostata	No	No	No	ND	Cx, Surg	AWD (?)
19	Vankarakunti (2006)	B (M)	Postauricular	No	No	No	ND	Surg	NED (12 mo)

Abbreviations: B, at birth; F, female; M, male; ND, not done; Cx, chemotherapy; Rx, radiotherapy; Surg, surgery; SCT, stem cell transplantation; DOD, die of disease; AWD; alive with disease; NED, no evidence of disease; d, day; w, week; mo, month; y, year.

LETTERS

Gain-of-function of mutated *C-CBL* tumour suppressor in myeloid neoplasms

Masashi Sanada^{1,5*}, Takahiro Suzuki^{7*}, Lee-Yung Shih^{8*}, Makoto Otsu⁹, Motohiro Kato^{1,2}, Satoshi Yamazaki⁶, Azusa Tamura¹, Hiroaki Honda¹¹, Mamiko Sakata-Yanagimoto¹², Keiki Kumano³, Hideaki Oda¹³, Tetsuya Yamagata¹⁴, Junko Takita^{1,2,3}, Noriko Gotoh¹⁰, Kumi Nakazaki^{1,4}, Norihiko Kawamata¹⁵, Masafumi Onodera¹⁶, Masaharu Nobuyoshi⁷, Yasuhide Hayashi¹⁷, Hiroshi Harada¹⁸, Mineo Kurokawa^{3,4}, Shigeru Chiba¹², Hiraku Mori¹⁸, Keiya Ozawa⁷, Mitsuhiro Omine¹⁸, Hisamaru Hirai^{3,4}, Hiromitsu Nakauchi^{6,9}, H. Phillip Koeffler¹⁵ & Seishi Ogawa^{1,5}

Acquired uniparental disomy (aUPD) is a common feature of cancer genomes, leading to loss of heterozygosity. aUPD is associated not only with loss-of-function mutations of tumour suppressor genes¹, but also with gain-of-function mutations of proto-oncogenes². Here we show unique gain-of-function mutations of the *C-CBL* (also known as *CBL*) tumour suppressor that are tightly associated with aUPD of the 11q arm in myeloid neoplasms showing myeloproliferative features. The *C-CBL* proto-oncogene, a cellular homologue of *v-Cbl*, encodes an E3 ubiquitin ligase and negatively regulates signal transduction of tyrosine kinases³⁻⁶. Homozygous *C-CBL* mutations were found in most 11q-aUPD-positive myeloid malignancies. Although the *C-CBL* mutations were oncogenic in NIH3T3 cells, *c-Cbl* was shown to functionally and genetically act as a tumour suppressor. *C-CBL* mutants did not have E3 ubiquitin ligase activity, but inhibited that of wild-type *C-CBL* and *CBL-B* (also known as *CBLB*), leading to prolonged activation of tyrosine kinases after cytokine stimulation. *c-Cbl*^{-/-} haematopoietic stem/progenitor cells (HSPCs) showed enhanced sensitivity to a variety of cytokines compared to *c-Cbl*^{+/+} HSPCs, and transduction of *C-CBL* mutants into *c-Cbl*^{-/-} HSPCs further augmented their sensitivities to a broader spectrum of cytokines, including stem-cell factor (SCF, also known as *KITLG*), thrombopoietin (TPO, also known as *THPO*), *IL3* and *FLT3* ligand (*FLT3LG*), indicating the presence of a gain-of-function that could not be attributed to a simple loss-of-function. The gain-of-function effects of *C-CBL* mutants on cytokine sensitivity of HSPCs largely disappeared in a *c-Cbl*^{+/+} background or by co-transduction of wild-type *C-CBL*, which suggests the pathogenic importance of loss of wild-type *C-CBL* alleles found in most cases of *C-CBL*-mutated myeloid neoplasms. Our findings provide a new insight into a role of gain-of-function mutations of a tumour suppressor associated with aUPD in the pathogenesis of some myeloid cancer subsets.

Myelodysplastic syndromes (MDS) are heterogeneous groups of blood cancers originating from haematopoietic precursors. They are

characterized by deregulated haematopoiesis showing a high propensity to acute myeloid leukaemia (AML)⁷. Some MDS cases have overlapping clinico-pathological features with myeloproliferative disorders, and are now classified into myelodysplasia/myeloproliferative neoplasms (MDS/MPN) by the World Health Organization (WHO) classification⁸. To obtain a comprehensive profile of allelic imbalances in these myeloid neoplasms, we performed allele-specific copy number analyses of bone marrow samples obtained from 222 patients with MDS, MDS/MPN, or other related myeloid neoplasms (Supplementary Tables 1 and 2) using high-density single nucleotide polymorphism (SNP) arrays combined with CNAG/AsCNAR software^{9,10}.

Genomic profiles of MDS and MDS/MPN showed characteristic unbalanced genetic changes, as reported in previous cytogenetic studies¹¹ (Supplementary Fig. 1a); however, they were detected more sensitively by SNP array analyses (Supplementary Table 3). aUPD was detected in 70 samples (31.5%) on the basis of the allele-specific copy number analyses, which substantially exceeded the detection rate obtained using a SNP call-based detection algorithm (20.7%) (Supplementary Figs 2 and 4, and Supplementary Tables 4 and 5). Long stretches of homozygous SNP calls caused by shared identical-by-descent alleles in parents were empirically predicted and excluded (Supplementary Fig. 3). aUPDs were more common in MDS/MPN than in MDS. They preferentially affected several chromosomal arms (1p, 1q, 4q, 7q, 11p, 11q, 14q, 17p and 21q) in distinct subsets of patients, and frequently associated with mutated oncogenes and tumour suppressor genes (Supplementary Figs 1b and 5). Among these, the most common aUPDs were those involving 11q (*n* = 17), which defined a unique subset of myeloid neoplasms that were clinically characterized by frequent diagnosis of chronic myelomonocytic leukaemia (CMML) with normal karyotypes (13 cases) (Fig. 1a and Supplementary Table 6). We identified a minimum overlapping aUPD segment of approximately 1.4 megabases (Mb) in 11q, which contained a mutated *C-CBL* proto-oncogene (Fig. 1b).

¹Cancer Genomics Project, ²Department of Pediatrics, ³Cell Therapy and Transplantation Medicine, and ⁴Hematology and Oncology, Graduate School of Medicine, The University of Tokyo, 7-3-1 Hongo, Bunkyo-ku, Tokyo 113-8655, Japan. ⁵Core Research for Evolutional Science and Technology, ⁶Exploratory Research for Advanced Technology, Japan Science and Technology Agency, 4-1-8 Honcho, Kawaguchi-shi, Saitama 332-0012, Japan. ⁷Division of Hematology, Department of Medicine, Jichi Medical University, 3311-1 Yakushiji, Shimotsuke-shi, Tochigi 329-0498, Japan. ⁸Division of Hematology-Oncology, Department of Internal Medicine, Chang Gung Memorial Hospital, Chang Gung University, 199 Tung Hwa North Road, Taipei 105, Taiwan. ⁹Division of Stem Cell Therapy, Center for Stem Cell and Regenerative Medicine. ¹⁰Division of Systems Biomedical Technology, Institute of Medical Science, The University of Tokyo, 4-6-1 Shirokanedai, Minato-ku, Tokyo 108-8639, Japan. ¹¹Department of Developmental Biology, Research Institute of Radiation Biology and Medicine, Hiroshima University, 1-2-3 Kasumi, Minami-ku, Hiroshima 734-8553, Japan. ¹²Department of Clinical and Experimental Hematology, Institute of Clinical Medicine, University of Tsukuba, 1-1-1 Tennodai, Tsukuba-shi, Ibaraki, 305-8571, Japan. ¹³Department of Pathology, Tokyo Women's Medical University, 8-1 Kawada-cho, Shinjuku-ku, Tokyo 162-8666, Japan. ¹⁴Department of Hematology, Dokkyo University School of Medicine, 800 Kitabayashi, Mibu, Tochigi 321-0293, Japan. ¹⁵Hematology/Oncology, Cedars-Sinai Medical Center, 8700 Beverly Boulevard, Los Angeles, California 90048, USA. ¹⁶Department of Genetics, National Research Institute for Child Health and Development, 2-10-1 Okura, Setagaya-ku, Tokyo, 157-8535, Japan. ¹⁷Gunma Children's Medical Center, 779 Shimohakoda, Hokkitsu-machi, Shibukawa-shi, Gunma 377-8577, Japan. ¹⁸Division of Hematology, Internal Medicine, Showa University Fujigaoka Hospital, 1-30 Fujigaoka, Aoba-ku, Yokohama, Kanagawa 227-8501, Japan.

*These authors contributed equally to this work.

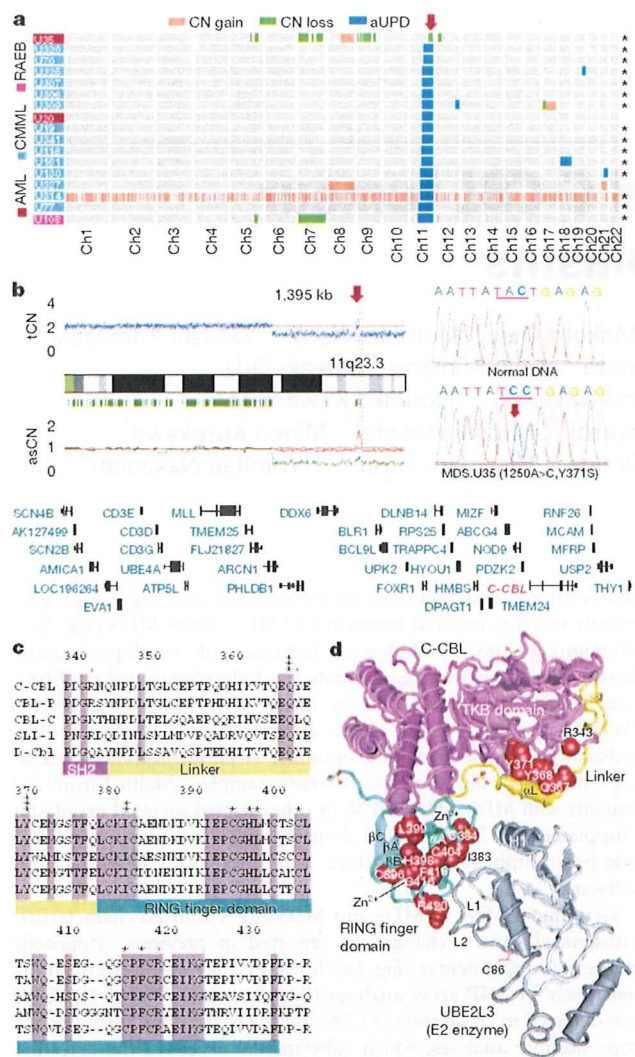


Figure 1 | Common UPD on the 11q arm and C-BL mutations in myeloid neoplasms. **a**, Copy number profiles of 17 cases with myeloid neoplasms showing 11qUPD. Regions of copy number (CN) gains, losses and aUPD are depicted in different colours. Histologies are shown by coloured boxes. Asterisks denote C-BL-mutated cases. Ch, chromosome; RAEB, refractory anaemia with excess blasts. **b**, CNAG output for MDS.U35. Total copy number (tCN) and allele-specific copy number (asCN) plots show a focal copy number gain spanning a 1.4-Mb segment within 3 Mb of an 11q-aUPD region (left), which contained mutated C-BL in MDS.U35 (right). **c**, Alignments of amino acid sequences for human CBL family proteins and their homologues in *Caenorhabditis elegans* (SLI-1) and *Drosophila* (D-Cbl). Amino acid numbering is on the basis of human C-BL. Conserved amino acids are highlighted. Positions of mutated amino acids are indicated by asterisks. Heterozygous mutations are shown in red. **d**, Mutated amino acid positions in the three-dimensional structure of a human C-BL-UBE2L3 complex. TKB, tyrosine kinase binding domain.

C-BL is the cellular homologue of the *v-Cbl* transforming gene of the Cas NS-1 murine leukaemia virus^{5,12}. It was recently found to be mutated in human AML cases^{13–15}. Together with its close homologue, CBL-B, C-BL is thought to be involved in the negative modulation of tyrosine kinase signalling, primarily through their E3 ubiquitin ligase activity that is responsible for the downregulation of activated tyrosine kinases^{3–5}. By sequencing all C-BL exons in all 222 samples, we found C-BL mutations in 15 of the 17 cases with 11q-aUPD, whereas only 3 out of 205 cases without 11q-aUPD had C-BL mutations, showing a strong association of C-BL mutations with 11q-aUPD ($P = 1.46 \times 10^{-18}$) (Supplementary Fig. 6 and

Supplementary Tables 6 and 7), as also indicated in a recent report¹⁶. Thus, C-BL was thought to be the major, if not the only, target of 11q-aUPD in myeloid neoplasms. Two different C-BL mutations co-existed in three cases (Supplementary Fig. 6b). Somatic origins of the mutations were confirmed in three evaluable cases (Supplementary Fig. 6c).

In most cases, C-BL mutations were missense, involving the evolutionarily conserved amino acids within the linker-RING finger domain that is central to the E3 ubiquitin ligase activity¹⁷ (Fig. 1c). Another case with a predominant Cys384Tyr mutation also contained a nonsense mutation (Arg343X) in a minor subclone, which resulted in a v-Cbl-like truncated protein (Supplementary Fig. 6b). In the remaining two cases, mutations led to amino acid deletions ($\Delta 369-371$ and $\Delta 368-382$) involving the highly conserved α -helix (αL) of the linker domain and the first loop of the RING finger. According to the published crystal structure of C-BL¹⁷, most of the mutated or deleted amino acids were positioned on the interface for the binding to the E2 enzyme (Fig. 1d), making contact with either the tyrosine kinase binding domain (Tyr 368 and Tyr 371) or E2 ubiquitin-conjugating enzymes (Ile 383, Cys 404 and Phe 418). Especially, all seven linker-domain mutations selectively involved just three amino acids (Gln367, Tyr368 and Tyr371) within the conserved αL helix (Fig. 1d). Mutations were clearly homozygous in nine cases, and the apparently heterozygous chromatograms in the other six cases could also be compatible with homozygous mutations affecting the aUPD-positive tumour clones, given the presence of substantial normal cell components within these samples. Mutations in the remaining three cases were considered to be heterozygous. About half of the C-BL-mutated cases carried coexisting mutations of RUNX1 (four cases), TP53 (one case), FLT3 internal tandem duplication (1 case) or JAK2 (3 cases). NRAS and KRAS mutations were prevalent among C-MML (15.1%) but occurred within discrete clusters from C-BL-mutated cases (Supplementary Tables 2 and 6 and Supplementary Fig. 5). The mutation status of C-BL did not substantially affect the clinical outcome (Supplementary Fig. 7).

All tested C-BL mutants induced clear oncogenic phenotypes in NIH3T3 fibroblasts, as demonstrated by enhanced colony formation in soft agar and tumour generation in nude mice (Supplementary Fig. 8). Transformed NIH3T3 cells showed PI3 kinase-dependent activation of Akt and the transformed phenotype was reverted by treatment with the PI3 kinase inhibitor Ly294002 (Supplementary Fig. 9). When introduced into Lin⁻ Sca1⁺ c-Kit⁺ (LSK) HSPCs, C-BL mutants (C-BL(Gln367Pro) and C-BL(Tyr371Ser)), as well as a mouse lymphoma-derived oncogenic mutant (C-BL(70Z)), significantly promoted the replating capacity of these progenitors (Fig. 2a). Because c-Cbl negatively modulates tyrosine kinase signalling, and all C-BL mutations, including those previously reported^{13–16}, affected the critical domains for its enzymatic activity involved in this modulation, C-BL was postulated to have a tumour suppressor function; loss-of-function could be a mechanism for the oncogenicity of these C-BL mutants^{3,5}. To assess this possibility and to clarify further the role of C-BL mutations in the pathogenesis of myeloid neoplasms, we generated *c-Cbl*^{-/-} mice and examined their haematological phenotypes (Supplementary Fig. 10).

In agreement with previous reports^{18–20}, *c-Cbl*^{-/-} mice exhibited splenomegaly and an augmented haematopoietic progenitor pool, as was evident from the increased colony formation of bone marrow cells in methylcellulose culture and higher numbers of LSK and CD34-negative LSK cells in bone marrow and/or spleen compared to their wild-type littermates (Fig. 2b–d and Supplementary Fig. 11). Furthermore, when introduced into a BCR-ABL transgenic background²¹, the *c-Cbl*^{-/-} allele accelerated blastic crisis depending on the allele dosage (Fig. 2e, f). These observations supported the notion that wild-type C-BL has tumour suppressor functions, whereas ‘mutant’ C-BL acts as an oncogene; C-BL can therefore be both a proto-oncogene and a tumour suppressor gene.

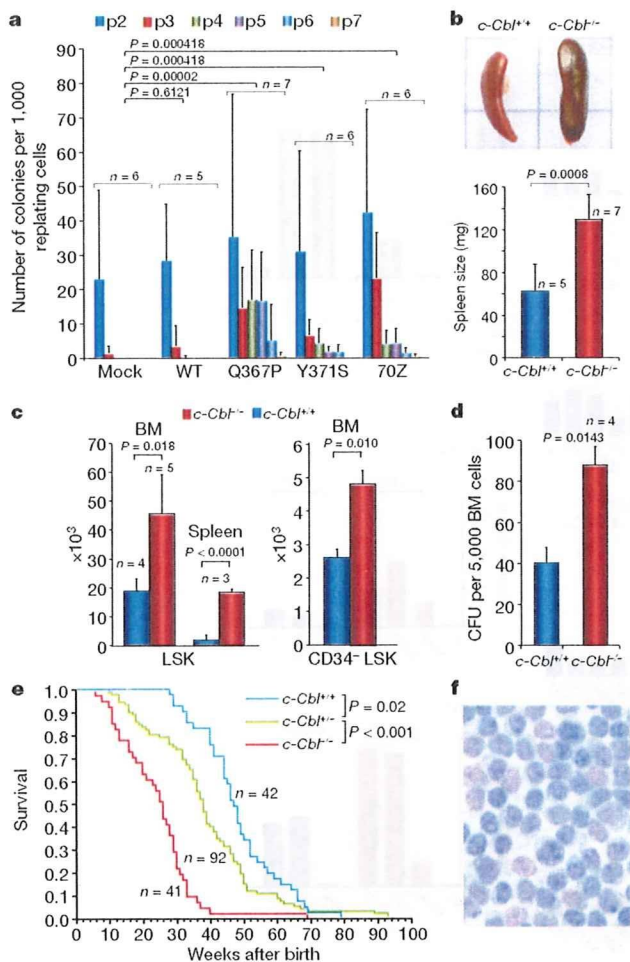


Figure 2 | Tumour-suppressor functions of wild-type C-CBL. **a**, Prolonged replating capacity of LSK cells transduced with mutant *C-CBL* (*C-CBL*(Gln367Pro) and *C-CBL*(Tyr371Ser)), compared to mock- or wild-type *C-CBL*-transduced cells. Replating capacity in methylcellulose culture is shown as mean colony number (and s.d.) per 1,000 replating cells at indicated times of replating, *p*, passage. **b**, Increased spleen mass in *c-Cbl*^{-/-} mice compared to *c-Cbl*^{+/+} mice (mean spleen weight and s.d.). **c**, Mean number of total LSK (left) and CD34-negative LSK (right) cells (plus s.d.) in bone marrow (BM) and/or spleen in *c-Cbl*^{+/+} (blue columns) and *c-Cbl*^{-/-} mice (red columns). Bone marrow cells from bilateral tibias and femurs were counted for each mouse. **d**, Augmented colony-forming potential of bone marrow cells from *c-Cbl*^{-/-} mice (mean colony number and s.d. per 5,000 bone marrow cells). CFU, colony-forming units. **e**, Kaplan-Meier survival curves of *c-Cbl*^{+/+}, *c-Cbl*^{+/+} and *c-Cbl*^{-/-} mice carrying a *BCR-ABL* transgene, showing acceleration of blastic crisis in *c-Cbl*^{+/+} and *c-Cbl*^{-/-} mice. **f**, Wright-Giemsa staining of an enlarged lymph node in a *Bcr-Abl*⁺ *c-Cbl*^{-/-} mouse during blastic crisis shows massive infiltrates of immature leukaemic blasts. Original magnification, $\times 600$.

Mouse LSK HSPCs expressed two Cbl family member proteins: wild-type *c-Cbl* and *Cbl-b* (Supplementary Fig. 12)²². When transduced into NIH3T3 cells stably expressing human epidermal growth factor receptor (EGFR), both Cbl proteins enhanced ubiquitination of EGFR after EGF stimulation, which was suppressed by coexpression of the *C-CBL* mutants (Fig. 3a, b). In haematopoietic cells, overexpression of wild-type *C-CBL* enhanced ligand-induced ubiquitination of a variety of tyrosine kinases, including *c-KIT*, *FLT3* and *JAK2*. In contrast, *C-CBL* mutants not only showed compromised enzymatic activity, but also inhibited the ubiquitinating activities in these haematopoietic cells (Fig. 3c), leading to prolonged tyrosine kinase activation after ligand stimulation (Fig. 3d).

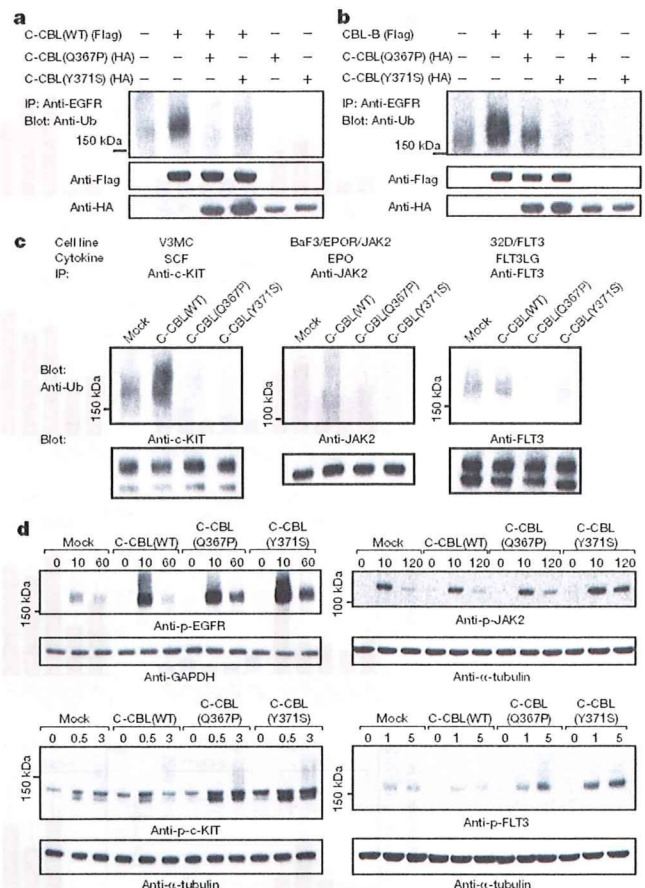


Figure 3 | Inhibitory actions of C-CBL mutants on wild-type C-CBL. **a**, **b**, Flag-tagged wild-type *C-CBL* (**a**) or *CBL-B* (**b**) were transfected into NIH3T3 cells stably transduced with human EGFR plus indicated HA-tagged *C-CBL* mutants. Anti-ubiquitin blots of immunoprecipitated EGFR after EGF stimulation show the inhibitory actions of the *C-CBL* mutants on ubiquitinating activity of *C-CBL* (**a**) and *CBL-B* (**b**). Bottom panels are anti-HA and anti-Flag blots of total cell lysates. **c**, Effects of wild-type and mutant *C-CBL* on cytokine-induced ubiquitination of *c-KIT*, *JAK2* and *FLT3* in haematopoietic cells V3MC, BaF3 co-transduced with human erythropoietin receptor (EPOR) and *JAK2* (BaF3/EPOR/*JAK2*), and *FLT3*-transduced 32D (32D/*FLT3*), respectively. Each cell line was further transduced with indicated *C-CBL* mutants, and ubiquitination of immunoprecipitated kinases was detected by anti-ubiquitin blots at 1 min after stimulation with SCF, EPO and *FLT3L*G. Anti-kinase blots of the precipitated kinases are shown below each panel. **d**, Kinase phosphorylation was examined at indicated time points (shown in minutes) after ligand stimulation using immunoblot analyses of total cell lysates using antibodies to phosphorylated (*p*-) EGFR, *c-KIT*, *JAK2* and *FLT3* in which anti- α -tubulin or anti-GAPDH blots are provided as a control.

Because tyrosine kinase signalling is central to cytokine responses in haematopoietic cells and its deregulation is a common feature of myeloproliferative disorders²³, we next examined the effects of *C-CBL* mutations (*C-CBL*(Gln367Pro) and *C-CBL*(Tyr371Ser)) and the loss of wild-type *C-CBL* alleles on the responses of LSK HSPCs to various cytokines. In serum-free conditions, *c-Cbl*^{-/-} LSK cells showed a modestly enhanced proliferative response to a variety of cytokines, including SCF, IL3 and TPO, compared to *c-Cbl*^{+/+} cells (mock columns in Fig. 4a). However, the enhanced response in *c-Cbl*^{-/-} cells was markedly augmented and extended to a broader spectrum of cytokines, including *FLT3* ligand by the transduction of *C-CBL* mutants. Of note, the effect of *C-CBL* mutant transduction was not remarkable in *c-Cbl*^{+/+} LSK cells except for the response to SCF, which was clearly enhanced by *C-CBL* mutants

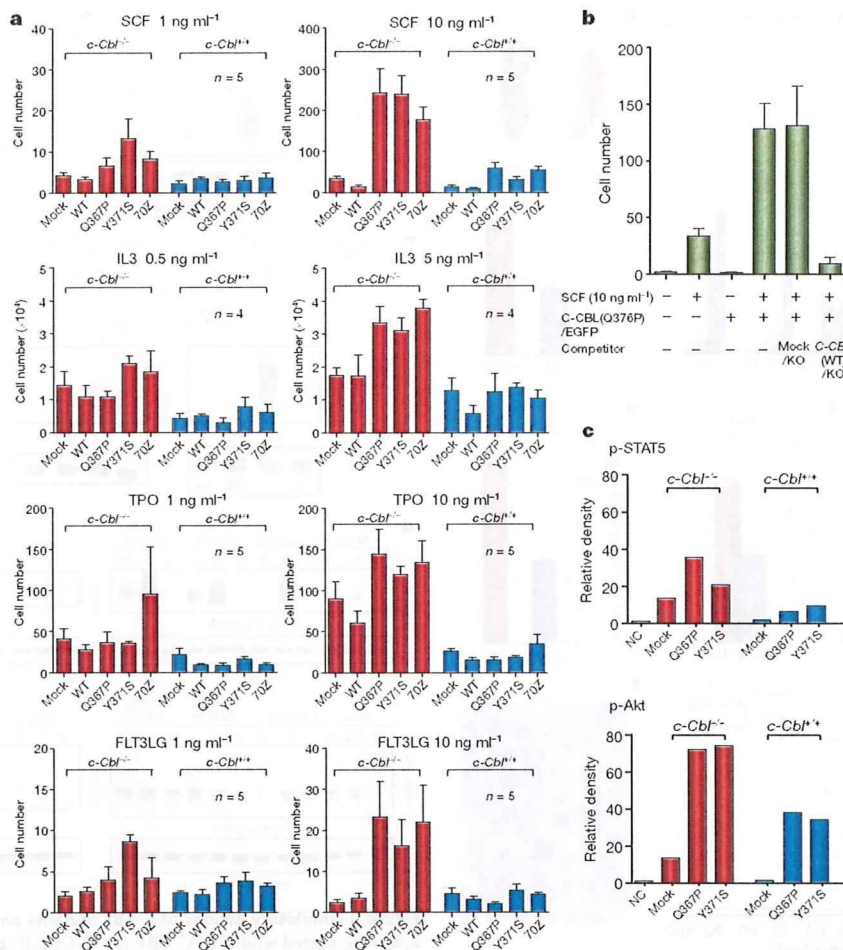


Figure 4 | Gain-of-function of mutant C-CBL augmented by loss of wild-type C-CBL. **a**, *c-Cbl*^{+/-} and *c-Cbl*^{-/-} LSK cells were transfected with various *C-CBL* internal ribosome entry site (IRES)/green fluorescent protein (GFP) constructs, and 50 GFP-positive cells were sorted for serum-free culture containing indicated concentrations of SCF, IL3, TPO and FLT3LG. Mean cell numbers (plus s.e.m.) on day 5 are plotted. **b**, *c-Cbl*^{-/-} LSK cells were co-transduced with *C-CBL*(Gln367Pro)-IRES-EGFP (*C-CBL*(Q367P)/EGFP) and mock-IRES-Kusabira-Orange (mock/KO) or wild-type *C-CBL*-IRES-Kusabira-Orange (*C-CBL*(WT)/KO), and 50 GFP/KO double-positive

even with a *c-Cbl*^{+/-} background (Fig. 4a and Supplementary Fig. 13). To clarify further the effect of wild-type *C-CBL* on *C-CBL* mutants, both wild-type *C-CBL* and *C-CBL* mutants were co-transduced into *c-Cbl*^{-/-} LSK cells, and their effects on the response to SCF were examined. As shown in Fig. 4b, the hyperproliferative response induced by *C-CBL* mutants was almost completely abolished by the co-transduction of wild-type *C-CBL*, suggesting the pathogenic importance of loss of wild-type *C-CBL* alleles found in most *C-CBL*-mutated cases. LSK cells transduced with *C-CBL* mutants also showed enhanced activation of the STAT5 and Akt pathways on cytokine stimulation (SCF and TPO), which was more pronounced in *c-Cbl*^{-/-} than *c-Cbl*^{+/-} LSK cells (Fig. 4c and Supplementary Fig. 14).

The modest enhancement of sensitivity to cytokines found in *c-Cbl*^{-/-} LSK cells was a consequence of loss of *C-CBL* functions. In contrast, the hypersensitive response of mutant-transduced *c-Cbl*^{-/-} LSK cells to a broad spectrum of cytokines represents gain-of-function of the mutants that could not be ascribed to a simple loss of *C-CBL* functions, which was also predicted from the strong association of *C-CBL* mutations with 11q-aUPD by analogy to the gain-of-function *JAK2* mutations associated with 9p-aUPD in polycythemia vera². The gain-of-function of *C-CBL* mutants became

cells were sorted into each well for cell proliferation assays in serum-free culture containing 10 ng ml⁻¹ SCF. Mean cell numbers on day 5 (plus s.e.m., *n* = 5) are plotted. **c**, Ten thousand *c-Cbl*^{+/-} and *c-Cbl*^{-/-} LSK cells transduced with various *C-CBL* constructs were stimulated with 10 ng ml⁻¹ SCF and 10 ng ml⁻¹ TPO for 15 min. Total cell lysates were analysed by immunoblotting, using antibodies to STAT5, Akt and their phosphorylated forms. The intensities of phosphorylated proteins relative to total STAT5 (top panel) and Akt (bottom panel) are plotted. NC indicates the mean background signal obtained with nonspecific IgG.

more evident under a *c-Cbl*^{-/-} background. The hypersensitive response to cytokines induced by mutant *C-CBL* under the *c-Cbl*^{-/-} background was largely offset by the presence of the wild-type *c-Cbl* allele or by the transduction of the wild-type *C-CBL* gene, suggesting that the gain-of-function could be closely related to loss of *C-CBL*-like functions, probably by inhibition of Cbl-b. Supporting this view is a previous report that *c-Cbl/Cbl-b* double knockout T cells showed more profound impairments in the downregulation of the T-cell receptor (TCR), more sustained TCR signalling, and more vigorous proliferation, than *c-Cbl* or *Cbl-b* single knockout T cells after anti-CD3 (also known as CD3e) stimulation²⁴. This is analogous to the gain-of-function found in some TP53 mutants, which has been explained by functional inhibition of two TP53 homologues, TP73 and TP63 (refs 25, 26). Of note, TP53 was also originally isolated as an oncogene through its mutated forms²⁷. The Cbl-b inhibition-based gain-of-function model could be tested directly by comparing the behaviour of *c-Cbl/Cbl-b* double knockout LSK cells with that of LSK cells carrying homozygously knocked-in mutant *C-CBL* alleles. On the other hand, there remains a possibility that the gain-of-function could be mediated by a mechanism other than the simple inhibition of the homologue, because *C-CBL* mutants retained several motifs

that interacted with numerous signal-transducing molecules. Furthermore, considering the ubiquitous expression of CBL proteins, it would be of interest to explore the possible involvement of mutations in all *CBL* family members in other human cancers.

METHODS SUMMARY

Genomic DNA from 222 bone marrow samples with myeloid neoplasms were analysed using GeneChip SNP-genotyping microarrays (Affymetrix GeneChip) as described². Allelic imbalances were detected from the allele-specific copy numbers calculated using CNAG/AsCNAR software (<http://www.genome.umin.jp>)^{9,10}. *C-CBL* mutations were examined by sequencing PCR-amplified genomic DNA. For functional assays, haemagglutinin (HA)- or Flag-tagged complementary DNAs of wild-type and mutant *C-CBL* were generated by *in vitro* mutagenesis, constructed into a MSCV-based retroviral vector, pGCDNsamIRESGFP or pGCDNsamIRESKO, and used for retrovirus-mediated gene transfer. For the evaluation of oncogenicity of *C-CBL* mutants, NIH3T3 cells were transfected with various *C-CBL* constructs and used for colony assays in soft agar and tumour formation assays in nude mice. *c-Cbl*-deficient mice were generated using a conventional strategy of gene-targeting and crossed with *BCR-ABL* transgenic mice to evaluate the effect of the *c-Cbl*^{-/-} allele on the acceleration of blastic crisis. LSK cells sorted from *c-Cbl*^{+/+} and *c-Cbl*^{-/-} mice were transduced with various *C-CBL* constructs. Their responses to cytokines were evaluated by cell proliferation assays, followed by immunoblot analyses of c-KIT, FLT3 and JAK2, as well as their downstream signalling molecules. The effects of *C-CBL* mutant expression on the ubiquitination of EGFR, c-KIT, FLT3 and JAK2 were examined by transducing *C-CBL* mutants into relevant cells, followed by anti-ubiquitin blots of the immunoprecipitated kinases after ligand stimulation. Functional competition of *C-CBL* mutants with wild-type *C-CBL* was assessed by cell proliferation assays of LSK cells co-transduced with both wild-type and mutant *C-CBL* genes. This study was approved by the ethics boards of the University of Tokyo, Chang Gung Memorial Hospital and Showa University. Antibodies and primers used in this study are listed in Supplementary Tables 8 and 9.

Full Methods and any associated references are available in the online version of the paper at www.nature.com/nature.

Received 9 October 2008; accepted 30 June 2009.

Published online 20 July 2009.

- Knudson, A. G. Two genetic hits (more or less) to cancer. *Nature Rev. Cancer* 1, 157–162 (2001).
- James, C. *et al.* A unique clonal JAK2 mutation leading to constitutive signalling causes polycythaemia vera. *Nature* 434, 1144–1148 (2005).
- Ryan, P. E. *et al.* Regulating the regulator: negative regulation of Cbl ubiquitin ligases. *Trends Biochem. Sci.* 31, 79–88 (2006).
- Schmidt, M. H. & Dikic, I. The Cbl interactome and its functions. *Nature Rev. Mol. Cell Biol.* 6, 907–918 (2005).
- Thien, C. B. & Langdon, W. Y. Cbl: many adaptations to regulate protein tyrosine kinases. *Nature Rev. Mol. Cell Biol.* 2, 294–307 (2001).
- Thien, C. B. & Langdon, W. Y. c-Cbl and Cbl-b ubiquitin ligases: substrate diversity and the negative regulation of signalling responses. *Biochem. J.* 391, 153–166 (2005).
- Corey, S. J. *et al.* Myelodysplastic syndromes: the complexity of stem-cell diseases. *Nature Rev. Cancer* 7, 118–129 (2007).
- Jaffe, E., Harris, N., Stein, H. & Vardiman J. *World Health Organization Classification of Tumours: Pathology and Genetics of Tumours of Haematopoietic and Lymphoid Tissues* 62–73 (IARC Press, 2002).
- Nannya, Y. *et al.* A robust algorithm for copy number detection using high-density oligonucleotide single nucleotide polymorphism genotyping arrays. *Cancer Res.* 65, 6071–6079 (2005).
- Yamamoto, G. *et al.* Highly sensitive method for genomewide detection of allelic composition in nonpaired, primary tumor specimens by use of affymetrix single-nucleotide-polymorphism genotyping microarrays. *Am. J. Hum. Genet.* 81, 114–126 (2007).
- Haase, D. Cytogenetic features in myelodysplastic syndromes. *Ann. Hematol.* 87, 515–526 (2008).
- Langdon, W. Y. *et al.* v-cbl, an oncogene from a dual-recombinant murine retrovirus that induces early B-lineage lymphomas. *Proc. Natl Acad. Sci. USA* 86, 1168–1172 (1989).
- Abbas, S. *et al.* Exon 8 splice site mutations in the gene encoding the E3-ligase CBL are associated with core binding factor acute myeloid leukemias. *Haematologica* 93, 1595–1597 (2008).
- Caligiuri, M. A. *et al.* Novel c-CBL and CBL-b ubiquitin ligase mutations in human acute myeloid leukemia. *Blood* 110, 1022–1024 (2007).
- Sargin, B. *et al.* FLT3-dependent transformation by inactivating c-Cbl mutations in AML. *Blood* 110, 1004–1012 (2007).
- Dunbar, A. J. *et al.* 250K single nucleotide polymorphism array karyotyping identifies acquired uniparental disomy and homozygous mutations, including novel missense substitutions of c-Cbl, in myeloid malignancies. *Cancer Res.* 68, 10349–10357 (2008).
- Zheng, N. *et al.* Structure of a c-Cbl-UbcH7 complex: RING domain function in ubiquitin-protein ligases. *Cell* 102, 533–539 (2000).
- Murphy, M. A. *et al.* Tissue hyperplasia and enhanced T-cell signalling via ZAP-70 in c-Cbl-deficient mice. *Mol. Cell Biol.* 18, 4872–4882 (1998).
- Naramura, M. *et al.* Altered thymic positive selection and intracellular signals in Cbl-deficient mice. *Proc. Natl Acad. Sci. USA* 95, 15547–15552 (1998).
- Rathinam, C. *et al.* The E3 ubiquitin ligase c-Cbl restricts development and functions of hematopoietic stem cells. *Genes Dev.* 22, 992–997 (2008).
- Honda, H. *et al.* Acquired loss of p53 induces blastic transformation in p210(bcr/abl)-expressing hematopoietic cells: a transgenic study for blast crisis of human CML. *Blood* 95, 1144–1150 (2000).
- Zeng, S. *et al.* Regulation of stem cell factor receptor signaling by Cbl family proteins (Cbl-b/c-Cbl). *Blood* 105, 226–232 (2005).
- Kaushansky, K. Hematopoietic growth factors, signaling and the chronic myeloproliferative disorders. *Cytokine Growth Factor Rev.* 17, 423–430 (2006).
- Naramura, M. *et al.* c-Cbl and Cbl-b regulate T cell responsiveness by promoting ligand-induced TCR down-modulation. *Nature Immunol.* 3, 1192–1199 (2002).
- Dittmer, D. *et al.* Gain of function mutations in p53. *Nature Genet.* 4, 42–46 (1993).
- Lang, G. A. *et al.* Gain of function of a p53 hot spot mutation in a mouse model of Li-Fraumeni syndrome. *Cell* 119, 861–872 (2004).
- Finlay, C. A., Hinds, P. W. & Levine, A. J. The p53 proto-oncogene can act as a suppressor of transformation. *Cell* 57, 1083–1093 (1989).
- Chen, Y. *et al.* Oncogenic mutations of ALK kinase in neuroblastoma. *Nature* 455, 971–974 (2008).

Supplementary Information is linked to the online version of the paper at www.nature.com/nature.

Acknowledgements This work was supported by the Core Research for Evolutional Science and Technology, Japan Science and Technology Agency, a Grant-in-Aid from the Ministry of Health, Labor and Welfare of Japan and from the Ministry of Education, Culture, Sports, Science and Technology, and a grant from National Health Research Institute, Taiwan, NHRI-EX96-9434SI, and NIH-2R01CA026038-30. We thank W. Y. Langdon for providing a human *C-CBL* cDNA. A mast-cell cell line expressing c-KIT V3MC was a gift from M. F. Gurish. We also thank Y. Ogino and K. Fujita for their technical assistance.

Author Contributions M.S. and M.Kato performed microarray experiments and subsequent data analyses. T.S., T.Y., H.Honda and H.Hirai generated and analysed *c-Cbl*-null mice. M.S., M.Otsu, S.Y., M.N., K.K., N.G., M.Onodera, M.S.-Y. and H.N. conducted functional assays of *C-CBL* mutants. L.-Y.S., M.S., M.Kato, K.N., J.T. and A.T. performed mutation analysis. H.O. performed pathological analysis of *c-Cbl*-null mice. L.-Y.S., N.K., H.Harada, M.Kurokawa, S.C., H.M., H.P.K. and M.Omine prepared MDS specimens. M.S., M.Otsu, Y.H., K.O., H.M., H.N., L.-Y.S., H.P.K. and S.O. designed the overall study, and S.O. wrote the manuscript. All authors discussed the results and commented on the manuscript.

Author Information Full copy number data for the 222 samples are accessible from the Gene Expression Omnibus public database (<http://ncbi.nlm.nih.gov/geo/>) with the accession number GSE15187. Reprints and permissions information is available at www.nature.com/reprints. Correspondence and requests for materials should be addressed to S.O. (sogawa-tky@umin.ac.jp) or L.-Y.S. (sly7012@adm.cgmh.org.tw).

METHODS

Genome-wide analysis of allelic imbalances in primary myeloid neoplasms. Bone marrow specimens were obtained from 222 patients diagnosed with myeloid neoplasms according to the WHO classification (Supplementary Tables 1 and 2). High molecular weight genomic DNA was extracted and used for microarray analysis using Affymetrix GeneChip 50K XbaI, HindIII or 250K NspI, according to the manufacturer's instructions. Genome-wide detection of allelic imbalances was performed using CNAG/AsCNAR software (<http://www.genome.umin.jp>)^{9,10}.

Mutation analysis. Mutation analysis was performed by direct sequencing of PCR-amplified coding exons of the relevant genes, using an ABI PRISM 3100 genetic analyser (Applied Biosystems). The target genes, exons and PCR primers are listed in Supplementary Table 8. Tandem duplication of the *FLT3* gene was examined by genomic PCR and sequencing.

Preparation of high-titre vesicular stomatitis virus glycoprotein (VSV-G)-pseudotyped retroviral particles. HA-tagged human *C-CBL* cDNA was a gift from W. Y. Langdon. Nine mutant cDNAs of *C-CBL*, including eight from patients' specimens and a 70Z mutant corresponding to a mutant isolated from mouse lymphoma²⁹, were generated on the basis of this construct, using a QuickChange site-directed mutagenesis kit (Stratagene). These were then constructed into the retrovirus vectors pGCDNsamIRESGFP and pGCDNsamIRESKO^{30,32}. Vector plasmids were co-transfected with a VSV-G cDNA into 293GP cells (provided by R. C. Mulligan) to obtain retrovirus-containing supernatant, which was then transduced into 293GPG cells to establish stable cell lines capable of producing VSV-G-pseudotyped retroviral particles on induction^{33,34}. The average titre of retrovirus stocks prepared from these cell lines routinely exceeded approximately $1-10 \times 10^7$ inclusion-forming units per ml, as estimated using Jurkat cells.

Assays for anchorage-independent growth and tumorigenicity in nude mice. NIH3T3 cells (the Japan Cell Resource Bank) were stably transduced with wild-type and mutant *C-CBL* by retrovirus-mediated gene transfer. For colony formation assays, 1.0×10^3 stable cells for each construct were inoculated in 0.33% top agar, and the numbers of colonies >1 mm in diameter were counted 3 weeks after inoculation ($n = 8$). Experiments were repeated four times. For tumour formation in nude mice, 1.0×10^7 stable cells were inoculated subcutaneously at two sites per mouse. Cells were inoculated at six sites in three mice for each construct.

Purification of LSK HSPCs. LSK HSPCs were purified from bone marrow and spleen as described^{35,36}. Multicolour flow cytometry analysis and cell sorting were performed using a MoFlo cell Sorter (Beckman Coulter). The purity of sorted cell fractions consistently exceeded 98%.

Replating assays of bone marrow progenitor cells. Bone marrow LSK cells were infected with IRES/GFP-containing retrovirus carrying mock, wild-type *C-CBL* and three *C-CBL* mutants (*C-CBL*(Gln367Pro), *C-CBL*(Tyr371Ser) and *C-CBL*(Cys384Gly)) as well as *C-CBL*(70Z) on RetroNectin-coated dishes. After 48 h infection in culture in StemSpan supplemented with SCF (50 ng ml⁻¹; Peprotech), TPO (20 ng ml⁻¹) and FLT3LG (20 ng ml⁻¹), 1.0×10^3 GFP-positive cells were inoculated in MethoCult M3231 supplemented with TPO (20 ng ml⁻¹), IL3 (10 ng ml⁻¹), IL6 (10 ng ml⁻¹), FLT3LG (10 ng ml⁻¹) and SCF (50 ng ml⁻¹) for colony formation. Colony-forming cells were collected 7 days after each inoculation, from which 1.0×10^5 cells were repeatedly subjected to replating until no colonies were produced. Experiments were repeated at the indicated times for each *C-CBL* construct.

Generation of *c-Cbl*^{-/-} mice and evaluation of their tumour-prone phenotype. *c-Cbl*^{-/-} mice were generated using a conventional method of gene targeting (Supplementary Fig. 10). *c-Cbl*^{+/+}, *c-Cbl*^{+/-} and *c-Cbl*^{-/-} mice were crossed with *BCR-ABL* transgenic mice, and their survival and the development of blastic crises were monitored.

Evaluation of haematopoietic pool size in *c-Cbl*^{-/-} mice. LSK and CD34⁺ LSK cells were sorted from bone marrow cells or spleens of *c-Cbl*^{-/-} mice, and their numbers were compared to those in *c-Cbl*^{+/+} littermates (8 week old). Approximately 5×10^3 bone marrow cells collected from *c-Cbl*^{+/+} and *c-Cbl*^{-/-} mice were inoculated into MethoCult M3231 culture supplemented with TPO (20 ng ml⁻¹), IL3 (10 ng ml⁻¹), IL6 (10 ng ml⁻¹), EPO (3 U ml⁻¹) and SCF (50 ng ml⁻¹). The number of colonies was counted 7 days after culturing.

In vitro cell proliferation assays. Approximately 6×10^5 LSK cells from *c-Cbl*^{-/-} mice and their *c-Cbl*^{+/+} littermates (8 week old) were sorted into RetroNectin-coated 96-well U-bottom plates containing α -minimum essential medium supplemented with 1% fetal bovine serum (FBS), mouse SCF (50 ng ml⁻¹), and human TPO (100 ng ml⁻¹). After 24 h pre-incubation, retrovirus supernatant was added to each well at a multiplicity of infection of about

10. The plates were incubated for another 24 h in the presence of protamine sulphate (10 μ g ml⁻¹), followed by repeated infection and extended culture for 2 days in S-Clone SF-O3 medium (Sanko Junyaku) supplemented with 1% BSA, 50 ng ml⁻¹ SCF and 50 ng ml⁻¹ TPO. On day 4, fluorescent-marker-positive cells were sorted for subsequent analyses. Cell survival and proliferation of LSK cells transduced with different *C-CBL* constructs were assessed in serum-free liquid culture in 96-well U-bottom plates in the presence of various cytokines. Each well received 50 fluorescent-marker-positive LSK cells, and the cells were cultured in S-Clone supplemented with 1% BSA plus SCF, TPO, IL3 or FLT3LG at the indicated concentrations. Cell numbers were counted either by analysing well images or by flow cytometry using FlowCount beads (Beckman Coulter). After 6 h serum starvation, 1×10^4 LSK cells transduced with various *C-CBL* constructs were stimulated with SCF (10 ng ml⁻¹) and TPO (10 ng ml⁻¹) for 15 min. Whole-cell lysates were examined for activation of STAT5 and Akt by immunoblots using the respective antibodies.

Immunoblot analysis of physical interactions between mutant *C-CBL* and *CBL-B*. Flag-tagged *CBL-B* or *C-CBL* was co-transfected into NIH3T3 cells with each of three HA-tagged *C-CBL* mutants (*C-CBL*(Gln367Pro), *C-CBL*(Tyr371Ser) and *C-CBL*(70Z)). Total cell lysates of these NIH3T3 cells were immunoprecipitated with anti-Flag antibody, followed by immunoblot analysis with anti-HA antibody.

Detection of ubiquitination and phosphorylation of kinases. After overnight serum starvation, NIH3T3 cells stably transduced with human EGFR, and indicated HA-tagged *C-CBL* mutants and Flag-tagged wild-type *C-CBL* were stimulated with human EGF (10 ng ml⁻¹) for 2 min. Cell lysates were immunoprecipitated with anti-EGF antibody, followed by immunoblotting using anti-ubiquitin antibody. Constructs for wild-type *C-CBL* and mutant *C-CBL* were stably transduced into a mast cell line, V3MC, FLT3-transduced 32D cells (32D/FLT3) and BaF3 cells transduced with human EPOR and JAK2 (BaF3/EPOR/JAK2) using retrovirus-mediated gene transfer. After overnight serum starvation, the transduced cells were stimulated with 10 ng ml⁻¹ SCF (V3MC), 10 U ml⁻¹ EPO (BaF3/EPOR/JAK2) or 10 ng ml⁻¹ FLT3LG (32D/FLT3) for 1 min. The specific kinases were immunoprecipitated with relevant antibodies, and their ubiquitination was detected by immunoblotting with anti-ubiquitin antibody. Tyrosine phosphorylation of EGFR, c-KIT, JAK2 and FLT3 was examined by immunoblot analyses of total cell lysates after cytokine stimulation at indicated time points, using antibodies specifically recognizing phosphorylated kinases, anti-p-EGFR, anti-p-c-KIT, anti-p-JAK2 and anti-p-FLT3, respectively. Anti-GAPDH or anti- α -tubulin immunoblot was performed as a control. Antibodies used in this study are listed in Supplementary Table 9.

Statistical analysis. Statistical significance of prolonged replating capacity of mutant *C-CBL*-transduced LSK cells was tested by counting the total number of dishes that produced colonies, followed by Fisher's exact test. Survival curves of *c-Cbl*^{+/+}, *c-Cbl*^{+/-} and *c-Cbl*^{-/-} mice containing the *BCR-ABL* transgene were generated using the Kaplan-Meier method. Overall survivals of *C-CBL*-mutated and non-mutated CMMML cases were analysed according to the proportional hazard model, using STATA software. Statistical differences in survival were evaluated using the log-rank test, and statistical differences in 2×2 contingency tables were tested according to Fisher's exact method. Student's *t*-tests were used to evaluate the significance of difference in spleen mass, number of haematopoietic progenitors and colony-forming cells between *c-Cbl*^{+/+} and *c-Cbl*^{-/-}.

29. Blake, T. J. *et al.* The sequences of the human and mouse *c-cbl* proto-oncogenes show *v-cbl* was generated by a large truncation encompassing a proline-rich domain and a leucine zipper-like motif. *Oncogene* 6, 653-657 (1991).
30. Hamanaka, S. *et al.* Stable transgene expression in mice generated from retrovirally transduced embryonic stem cells. *Mol. Ther.* 15, 560-565 (2007).
31. Nabekura, T. *et al.* Potent vaccine therapy with dendritic cells genetically modified by the gene-silencing-resistant retroviral vector GCDNsap. *Mol. Ther.* 13, 301-309 (2006).
32. Sanuki, S. *et al.* A new red fluorescent protein that allows efficient marking of murine hematopoietic stem cells. *J. Gene Med.* 10, 965-971 (2008).
33. Ory, D. S., Neugeboren, B. A. & Mulligan, R. C. A stable human-derived packaging cell line for production of high titer retrovirus/vesicular stomatitis virus G pseudotypes. *Proc. Natl. Acad. Sci. USA* 93, 11400-11406 (1996).
34. Suzuki, A. *et al.* Feasibility of *ex vivo* gene therapy for neurological disorders using the new retroviral vector GCDNsap packaged in the vesicular stomatitis virus G protein. *J. Neurochem.* 82, 953-960 (2002).
35. Ema, H. *et al.* Adult mouse hematopoietic stem cells: purification and single-cell assays *Nature Protoc.* 1, 2979-2987 (2006).
36. Osawa, M. *et al.* Long-term lymphohematopoietic reconstitution by a single CD34-low/negative hematopoietic stem cell. *Science* 273, 242-245 (1996).

CASE REPORT

Acute megakaryoblastic leukemia in a child with the *MLL-AF4* fusion gene

Junko Takita^{1,2,3}, Ai Motomura², Katsuyoshi Koh², Kohmei Ida², Tomohiko Taki⁴, Yasuhide Hayashi⁵, Takashi Igarashi²

¹Department of Cell Therapy and Transplantation Medicine, ²Department of Pediatrics, ³Department of Cancer Genomics Project, Graduate School of Medicine, University of Tokyo, Tokyo; ⁴Department of Molecular Laboratory Medicine, Kyoto Prefectural University of Medicine, Graduate School of Medical Science, Kyoto; ⁵Gunma Children's Medical Centre, Gunma, Japan

Abstract

Mixed-lineage leukemia (*MLL*) rearrangements are commonly observed in childhood acute lymphoblastic and myeloid leukemia, as well as therapy-related leukemia. However, the occurrence of *MLL* rearrangements in acute megakaryoblastic leukemia (AMKL) is very rare. We report a pediatric case of AMKL with the *MLL-AF4* fusion transcript. *MLL-AF4* is derived from t(4;11)(q21;q23) and occurs exclusively in B-cell lineage leukemia. To our knowledge, *MLL-AF4* as well as t(4;11)(q21;q23) has not been reported in adult and childhood AMKL. Thus, our case provides new insight into the molecular mechanisms of *MLL-AF4*-associated leukemia.

Key words acute megakaryoblastic leukemia; 11q23 rearrangement; *MLL-AF4*

Correspondence Junko Takita, MD, PhD, Department of Cell Therapy and Transplantation Medicine, Graduate School of Medicine, University of Tokyo, 7-3-1, Hongo, Bunkyo-ku, 113-8655 Tokyo, Japan. Tel.: +81 (3) 3815 5411 (Ex 33462); Fax: +81 (3) 3816 4108; e-mail jtakita-ky@umin.ac.jp

Accepted for publication 29 April 2009

doi:10.1111/j.1600-0609.2009.01275.x

Acute megakaryoblastic leukemia (AMKL) is a heterogeneous subgroup of acute myeloid leukemia (AML) and recognized as AML M7 according to the French-American-British (FAB) cooperative group classification system (1). Previous studies on clinicopathological analyzes of AML suggest that AMKL is relatively rare, approximately 5–10% of all AML (2). Childhood AMKL is the most common form of Down syndrome-related leukemia, and its prognosis is excellent in this group of patients (2). AMKL without Down syndrome appears to be more heterogeneous, and its prognostic factors have not been well defined (3). The t(1;22)(p13;q13) translocation forming the chimeric fusion transcript, *OTT-MAL*, is the most common chromosomal abnormality in infants with AMKL who do not have Down syndrome (4, 5). Infants with AMKL and this translocation usually have abdominal masses, myelofibrosis, and a relatively poor prognosis (6). However, other molecular genetic mechanisms in children with AMKL without Down syndrome are still elusive.

Chromosomal rearrangement of 11q23 involving the mixed-lineage leukemia (*MLL*) gene is commonly found in childhood lymphoid, myeloid, and *MLLs* (7). Recent cytogenetic and molecular studies have shown that *MLL* has more than 50 different partner genes, including *AF4* at 4q21, *AF9* at 9p21, *AF10* at 10p21, and *ENL/ELL* at 19p13 (7). The most frequent 11q23 abnormality in AML is t(9;11)(p22;q23); other common abnormalities include t(11;19)(q23;p13.3) and t(11;19)(q23;q13.1) (8). More than 15 additional aberrations on 11q23 with various partners, including t(6;11), t(10;11), and t(11;17), have been reported in AML (8, 9). These 11q23 aberrations mainly occur in AML M4 and M5 and are rare in AMKL (8, 10, 11).

Of the various partners, *AF4* at 4q21 is the most common partner for *MLL*, and the *MLL-AF4* fusion transcript has been detected almost exclusively in B-cell lineage leukemia (12). Involvement of the *MLL-AF4* fusion transcript in *de novo* myeloid-lineage leukemia is known to be very rare (3). We describe the first case

of a child with AMKL with the *MLL-AF4* fusion gene.

Case report

A 3-year-old girl presented with fever and epistaxis and admitted to our hospital in January 2004. Physical examination showed anemia, hepatosplenomegaly, and petechiae on the trunk and extremities. Cervical, axillary, and inguinal lymph nodes were negligible. A peripheral blood cell count showed a white blood cell count of 6100/ μ L, with 34% mature granulocytes, 9% monocytes, 1% eosinophils, 38% lymphocytes, and 18% blasts. The hemoglobin concentration was 9.7 g/dL, and the platelet count was 14 000/ μ L. Bone marrow aspiration showed myeloid hyperplasia with 6% myeloid cells, 4.5% erythroid cells, 22% lymphoid cells, 0.5% monocyte cells, and 76% blasts (Fig. 1A). Blast cells were negative for peroxidase staining, and Auer rods were not found in the blasts. Approximately 40% of the blasts had cytoplasmic blebs (Fig. 1A). Immunophenotyping showed that blasts

expressed the CD7, CD13, CD33, CD34, and CD41a antigens, and a diagnosis of AMKL (AML M7) was made. Chemotherapy following the Japanese Childhood AML Cooperative Study Group Protocol, AML99, for intermediate-risk AML (cytarabine, idarubicin, etoposide, and mitoxantrone) induced complete clinical and cytogenetic remission. Thereafter, the patient underwent six courses of intensification chemotherapy; however, hematological relapse occurred 2 months later. Although chemotherapy according to the AML99 protocol and the FLAG (fludarabin, cytarabine, and G-CSF) regimen was provided, the disease progressed, and the patient died 12 months after diagnosis. Informed consent for the genetic analyzes of leukemic cells from this patient was obtained from the parents.

Cytogenetic studies

Chromosomal analyzes of leukemic blasts were performed at initial diagnosis, remission, and relapse using standard G-banding methods (13). Bone marrow blasts

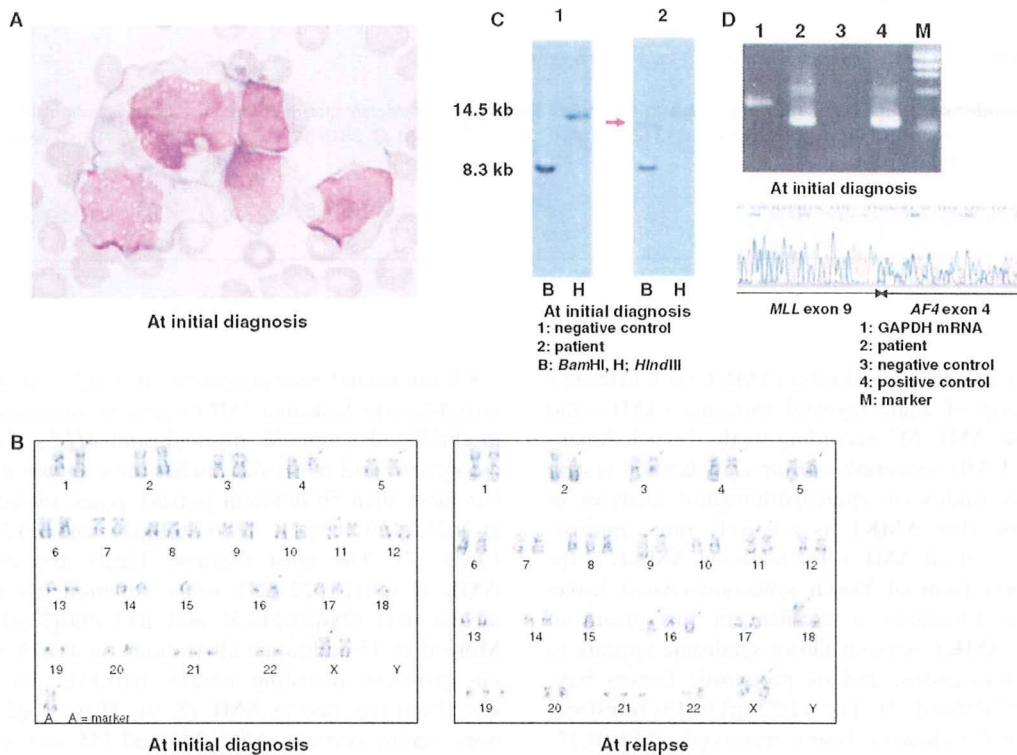


Figure 1 Morphological and cytogenetic analyzes of leukemic cells from the patient. (A) May-Giemsa staining of bone marrow cells at initial diagnosis. The blasts had cytoplasmic blebs. (B) Karyotypic findings in the patient. Complex chromosomal aberrations, including add(X)(q26), add(4)(q21), del(5)(q23q32), +8, del(11)(q23), -15, add(16)(q22), -18, and +21, were detected in bone marrow aspirates at the time of initial diagnosis (left) and at relapse (right). (C) Southern blot analysis of the blasts at the time of initial diagnosis with an *MLL* cDNA probe, which showed the rearrangement of *MLL* with *Bam*HI digestion (arrowhead). (D) RT-PCR analysis of the *MLL-AF4* fusion transcript in the blast at the time of initial diagnosis. A direct sequencing of the clear band identified the fusion of exon 9 of the *MLL* and exon 4 of the *AF4*. A direct sequencing of the faint band identified the fusion of exon 9 of the *MLL* and exon 4, which was considered to be generated by alternative splicing.

at initial diagnosis and relapse showed complex chromosomal aberrations as follow: 47~48, X, add(X)(q26), add(1)(q32), add(1), add(4)(q21), del(5)(q23q32), +8, del(11)(q23), -15, add(16)(q22), -18, +19, +21, +mar, inc. (in eight cells of 20 investigated, at initial diagnosis) and 49~50, X, add(X)(q26), del(2)(q11), t(3;9)(q21;q34), add(4)(q21), del(5)(q23q32), +8, del(11)(q23), -15, add(16)(q22), t(1;16)(q25;q22), add(17)(p11), add(18)(p11), -18, +19, +21 (in all 20 cells investigated, at relapse) (Fig. 1B).

These complex chromosomal aberrations commonly including add(X)(q26), add(4)(q21), del(5)(q23q32), +8, -15, del(11)(q23), +18, and +21 in 24 of 40 cells investigated (Fig.1B). Although trisomy 21 was commonly observed in the blast cells, chromosomal analysis of the bone marrow aspiration at remission exhibited a normal karyotype, 46XX, which indicated that the patient did not have Down syndrome.

Genetic analyzes

With an overall frequency of 15%, abnormalities of 11q23 are among the most frequent chromosomal aberrations in childhood AML, and recent molecular investigations of well-known 11q23 translocation have shown consistent involvement of the *MLL* gene (7). Therefore, because the cytogenetic studies conducted at the time of diagnosis and relapse in the bone marrow aspirate of this patient detected the common cytogenetic aberration del(11)(q23), we further investigated the status of the *MLL* gene in leukemic cells of this patient. Southern blot analysis using an *MLL* cDNA probe showed rearrangement of the *MLL* gene with *Bam*HI digestion (Fig. 1C). To identify the partner gene fused to *MLL*, we focused on the common chromosomal aberration add(4)(q21), because the *AF4* gene at 4q21 is one of the most common partner genes of *MLL* (7). RT-PCR analysis using the sense primer located in exon 8 of *MLL* and the anti-sense primer located in exon 6 of *AF4* showed the *MLL-AF4* transcript (Fig. 1D). The *OTT-MAL* fusion gene derived from t(1;22)(p13;q13) is predominantly detected in non-Down cases with AMKL; however, this fusion transcript was not detected in our case. In addition, although a mutational analysis of the *FLT3* and *GATA1* genes was performed as described previously (14), no mutations were detected in leukemic cells of these patients.

Discussion

Chromosomal translocations involving the *MLL* gene at chromosome 11q23 are often associated with the phenotype for acute leukemia (7). For instance, *MLL* rearrangements are commonly found in infant acute

lymphoblastic leukemia (ALL) and childhood *de novo* AML and in most patients with therapy-related leukemia (7). AML patients with *MLL* rearrangement tend to be young and often have hyperleukocytosis and myelomonocytic (FAB M4) or monoblastic (FAB M5) disease (3). However, the occurrence of the *MLL* rearrangement in AMKL (FAB M7) is very rare and limited to children (3, 8). To the best of our knowledge, only 16 cases of AMKL with *MLL* and/or 11q23 involvement have been reported (Table 1) (8, 9, 15). Thirteen of these 16 cases had *MLL* rearrangements, as detected by molecular studies; however, *MLL-AF4* fusion, t(4;11)(q21;q23) abnormalities, and abnormalities at 4q21 were not shown (8, 9, 15). The *MLL-AF4* fusion is the most commonly detected gene in infant ALL and appears to represent approximately 5% of ALL in older children and adults (16). Moreover, using conventional knockin or conditional inverter approaches, Mll-Af4 is capable of inducing B-cell lymphoma in mice models (17). However, our case suggests that *MLL-AF4* fusion is not exclusively associated with lymphoid malignancies.

Although rearrangements of 11q23 confer a poor prognosis in childhood ALL, the prognostic significance of 11q23 abnormalities in childhood AML is equivocal (7). Seven of 16 previously reported AMKL cases with 11q23 rearrangement and current case died, and one case relapsed 2 months after bone marrow transplantation (Table 1).

Previously it has been reported that a complex karyotype with multiple chromosomal abnormalities at diagnosis in AMKL would be a poor prognostic indicator (2). Interestingly, 12 of 16 previously reported AMKL cases with 11q23 aberrations and our case had variable complex karyotypes (Table 1). Thus, patients with AMKL with 11q23 aberrations tend to have a poor prognosis may be due to the complex karyotypes. Furthermore, of the 17 cases with AMKL with 11q23 aberrations (including our case), 15 cases were not associated with Down syndrome, and the status of the remaining two was unknown (8, 9, 15). These clinical and cytogenetic data suggest that childhood AMKL with 11q23 abnormalities might be a specific subtype of AMKL with a complex karyotype and poor prognosis and is not associated with Down syndrome. Allogenic bone marrow transplantation could be the best treatment for this group patients, but the too few number of case prevent to compare.

Although cytogenetic studies of leukemic cells of the present case showed common del(11)(q23) and add(4)(q21) abnormalities, the karyotypes shown in this case does not suggest it as a typical t(4;11) translocation. Because translocations of 11q23 are often not detected by standard G-banding methods, the frequency of *MLL* involvement in AMKL is still probably underestimated. Therefore, a combination of cytogenetic and molecular

Table 1 Acute megakaryoblastic leukemia with 11q23 and/or the *MLL* rearrangement

Case no.	Age (years)	Karyotype	<i>MLL</i> status	Outcome	Reference
1	2	49,XX,+6,t(10;11)(p13;q23),+21,+22	nd	Dead	(16)
2 ¹	nd	50,XX,+6,+8,t(9;11)(p21;q23),+20,+21	nd	nd	(16)
3	nd	46,XX,t(9;11)(p21;q23)	nd	Alive ²	(16)
4	12	51,XX,+6,+15,+17,+20,+21	<i>MLL-AF10</i>	Dead	(16)
5	5	52,XX,+X,+3,t(9;11)(p22;q23),+12,+15,+19,+21	R	Alive ²	(16)
6	1	54,XX,del(3)(q13q21),+6,+7,+8,t(11;17)(q23;q23),+14,+19,+19,+21,+21	R	Alive	(16)
7	15	46,XX,t(9;11)(p22;q23) [6]/47,idem,+6[7]/92,idemx2[2]/94,idemx2,+6,+6[5]	R	nd	(16)
8	1	t(5;9;11)(q33;p22;q23)	R	Dead	(9)
9	1.9	50,XX,+der(6)t(6;10;11)(q10;p10-12;q22-23),der(7)t(7;11)(p15;q23),der(10)ins(10;11)(p13;q22-23),der(11)t(7;11)ins(10;11),add(16)(q24),+19,+21,+22	R	Dead	(9)
10	2	51,X,t(X;11)(q22;q23),+6,+8,+19,+21,+21	R	Dead	(9)
11	0.7	48,Y,+X,t(X;19)(q26;q13),der(10)del(10)(p13)t(10;20;16)(q23;q11;p13),ins(15;5)(q11;q11q13),der(16)t(10;20;16),+19,der(20)t(10;20;16)	R	Dead	(9)
12	4.9	46,XX,t(7;11)(q22;p15)	R	Dead	(9)
13	15	92,XXXX,t(9;11)(p22;q23)[2]/94,XXXX,+6,+6,t(9;11)[5]/47,XX,+6,t(9;11)[7]	R	Alive ²	(16)
14	2	47,XY,der(4)(?::4p15 → 4qter),der(6)(6pter → 6q22::11q? → 11q?::4p15 → 4pter),der(10)(6qter → 6q26::15q21 → 15q24::11q2? → 11q23::10p12 → 10qter),del(11)(q14),der(15)(15pter → 15q21::6q22 → 6q26::10p12 → 10pl?::18q11.2 → 18qter),der(18)(18pter → 18q11.2::15q24 → 15qter),+21	<i>MLL-AF10</i>	Relapse at 2 m from BMT	
15	nd	nd	<i>MLL-AF10</i>	Alive	(15)
16	nd	nd	<i>MLL-ENL</i>	Alive	(15)
17	3.6	47~48,X,add(X)(q26),add(1)(q32),add(1),add(4)(q21),del(5)(q23q32),+8,del(11)(q23),-15,add(16)(q22),-18,+19,+21,+mar,inc, (at diagnosis) 49~50,X,add(X)(q26),del(2)(q11),t(3;9)(q21;q34),add(4)(q21),del(5)(q23q32),+8,del(11)(q23),-15,add(16)(q22),t(1;16)(q25;q22),add(17)(p11),add(18)(p11),-18,+19,+21 (at relapse)	<i>MLL-AF4</i> <i>MLL-AF4</i>	Dead	Present case

R, rearranged; nd, not determined; m, months; BMT, bone marrow transplantation; AMKL, acute megakaryoblastic leukemia.

¹Therapy-related AMKL.

²Short follow-up.

studies, such as Southern blot and RT-PCR analyzes, is better at identifying *MLL* involvement.

The *OTT-MAL* fusion transcript is closely associated with non-Down AMKL in infants, and the *GATA1* mutations are frequently detected in AMKL with Down syndrome (18). However, the *OTT-MAL* and *GATA1* mutations were not detected in our patient, which suggested that her disease was an independent subgroup of childhood AMKLs. Furthermore, *FLT3* is one of the most commonly mutated genes in AML, and AML patients with the *FLT3* mutation usually have a poor prognosis (19). In our patient, no *FLT3* mutation was detected, indicating that a pathway other than *FLT3* signaling would have existed in her aggressive disease. Because the prog-

nostic factors for non-Down AML in children are still unclear, further data accumulation is necessary.

Acknowledgements

We thank Mrs Sohma, Mrs Matsumura, Ms Sato and Dr Yokota for their excellent technical assistance. This work was supported by Research on Measures for Intractable Diseases, Health and Labor, Sciences Research Grants, Ministry of Health, Labor and Welfare, by Research on Health Sciences focusing on Drug Innovation, by the Japan Health Sciences Foundation, and by Core Research for Evolutional Science and Technology, Japan Science and Technology Agency.

References

- Bennett JM, Catovsky D, Daniel MT, *et al.* Criteria for the diagnosis of acute leukemia of megakaryocyte lineage (M7). A report of the French-American-British Cooperative Group. *Ann Intern Med* 1985;103:460-2.
- Dastugue N, Lafage-Pochitaloff M, Pages MP, *et al.* Cytogenetic profile of childhood and adult megakaryoblastic leukemia (M7): a study of the Groupe Francais de Cytogenetique Hematologique (GFCH). *Blood* 2002;100:618-26.
- Paredes-Aguilera R, Romero-Guzman L, Lopez-Santiago N, *et al.* Biology, clinical, and hematologic features of acute megakaryoblastic leukemia in children. *Am J Hematol* 2003;73:71-80.
- Trejo RM, Aguilera RP, Nieto S, *et al.* A t(1;22)(p13;q13) in four children with acute megakaryoblastic leukemia (M7), two with Down syndrome. *Cancer Genet Cytogenet* 2000;120:160-2.
- Mercher T, Coniat MB, Monni R, *et al.* Involvement of a human gene related to the *Drosophila* *spen* gene in the recurrent t(1;22) translocation of acute megakaryocytic leukemia. *Proc Natl Acad Sci USA* 2001;98:5776-9.
- Isaacs H Jr. Fetal and neonatal leukemia. *J Pediatr Hematol Oncol* 2003;25:348-61.
- Meyer C, Schneider B, Jakob S, *et al.* The *MLL* recombinome of acute leukemias. *Leukemia* 2006;20:777-84.
- Shih LY, Liang DC, Fu JF, *et al.* Characterization of fusion partner genes in 114 patients with de novo acute myeloid leukemia and *MLL* rearrangement. *Leukemia* 2006;20:218-23.
- Rubnitz JE, Raimondi SC, Tong X, *et al.* Favorable impact of the t(9;11) in childhood acute myeloid leukemia. *J Clin Oncol* 2002;20:2302-9.
- Chaplin T, Bernard O, Beverloo HB, *et al.* The t(10;11) translocation in acute myeloid leukemia (M5) consistently fuses the leucine zipper motif of *AF10* onto the *HRX* gene. *Blood* 1995;86:2073-6.
- Martineau M, Berger R, Lillington DM, *et al.* The t(6;11)(q27;q23) translocation in acute leukemia: a laboratory and clinical study of 30 cases. EU Concerted Action 11q23 Workshop participants. *Leukemia* 1998;12:788-91.
- Heerema NA, Sather HN, Ge J, *et al.* Cytogenetic studies of infant acute lymphoblastic leukemia: poor prognosis of infants with t(4;11) - a report of the Children's Cancer Group. *Leukemia* 1999;13:679-86.
- Hayashi Y, Hanada R, Yamamoto K. Chromosome abnormalities and prognosis in childhood acute leukemia. *Acta Paediatr Jpn* 1991;33:497-506.
- Kawamura M, Kaku H, Taketani T, *et al.* Mutations of *GATA1*, *FLT3*, *MLL*-partial tandem duplication, *NRAS*, and *RUNX1* genes are not found in a 7-year-old Down syndrome patient with acute myeloid leukemia (FAB-M2) having a good prognosis. *Cancer Genet Cytogenet* 2008;180:74-8.
- Morello C, Rapella A, Tassano E, *et al.* *MLL-MLLT10* fusion gene in pediatric acute megakaryoblastic leukemia. *Leuk Res* 2005;29:1223-6.
- Meyer C, Kowarz E, Schneider B, *et al.* Genomic DNA of leukemic patients: target for clinical diagnosis of *MLL* rearrangements. *Biotechnol J* 2006;1:656-63.
- Chen W, Li Q, Hudson WA, *et al.* A murine *MLL-AF4* knock-in model results in lymphoid and myeloid deregulation and hematologic malignancy. *Blood* 2006;108:669-77.
- Wechsler J, Greene M, McDevitt MA, *et al.* Acquired mutations in *GATA1* in the megakaryoblastic leukemia of Down syndrome. *Nat Genet* 2002;32:148-52.
- Gilliland DG, Griffin JD. The roles of *FLT3* in hematopoiesis and leukemia. *Blood* 2002;100:1532-42.

LETTERS

Frequent inactivation of A20 in B-cell lymphomas

Motohiro Kato^{1,2}, Masashi Sanada^{1,5}, Itaru Kato⁶, Yasuharu Sato⁷, Junko Takita^{1,2,3}, Kengo Takeuchi⁸, Akira Niwa⁶, Yuyan Chen^{1,2}, Kumi Nakazaki^{1,4,5}, Junko Nomoto⁹, Yoshitaka Asakura⁹, Satsuki Muto¹, Azusa Tamura¹, Mitsuru Iio¹, Yoshiki Akatsuka¹¹, Yasuhide Hayashi¹², Hiraku Mori¹³, Takashi Igarashi², Mineo Kurokawa⁴, Shigeru Chiba³, Shigeo Mori¹⁴, Yuichi Ishikawa⁸, Koji Okamoto¹⁰, Kensei Tobinai⁹, Hitoshi Nakagama¹⁰, Tatsutoshi Nakahata⁶, Tadashi Yoshino⁷, Yukio Kobayashi⁹ & Seishi Ogawa^{1,5}

A20 is a negative regulator of the NF- κ B pathway and was initially identified as being rapidly induced after tumour-necrosis factor- α stimulation¹. It has a pivotal role in regulation of the immune response and prevents excessive activation of NF- κ B in response to a variety of external stimuli²⁻⁷; recent genetic studies have disclosed putative associations of polymorphic A20 (also called *TNFAIP3*) alleles with autoimmune disease risk^{8,9}. However, the involvement of A20 in the development of human cancers is unknown. Here we show, using a genome-wide analysis of genetic lesions in 238 B-cell lymphomas, that A20 is a common genetic target in B-lineage lymphomas. A20 is frequently inactivated by somatic mutations and/or deletions in mucosa-associated tissue lymphoma (18 out of 87; 21.8%) and Hodgkin's lymphoma of nodular sclerosis histology (5 out of 15; 33.3%), and, to a lesser extent, in other B-lineage lymphomas. When re-expressed in a lymphoma-derived cell line with no functional A20 alleles, wild-type A20, but not mutant A20, resulted in suppression of cell growth and induction of apoptosis, accompanied by downregulation of NF- κ B activation. The A20-deficient cells stably generated tumours in immunodeficient mice, whereas the tumorigenicity was effectively suppressed by re-expression of A20. In A20-deficient cells, suppression of both cell growth and NF- κ B activity due to re-expression of A20 depended, at least partly, on cell-surface-receptor signalling, including the tumour-necrosis factor receptor. Considering the physiological function of A20 in the negative modulation of NF- κ B activation induced by multiple upstream stimuli, our findings indicate that uncontrolled signalling of NF- κ B caused by loss of A20 function is involved in the pathogenesis of subsets of B-lineage lymphomas.

Malignant lymphomas of B-cell lineages are mature lymphoid neoplasms that arise from various lymphoid tissues^{10,11}. To obtain a comprehensive registry of genetic lesions in B-lineage lymphomas, we performed a single nucleotide polymorphism (SNP) array analysis of 238 primary B-cell lymphoma specimens of different histologies, including 64 samples of diffuse large B-cell lymphomas (DLBCLs), 52 follicular lymphomas, 35 mantle cell lymphomas (MCLs), and 87 mucosa-associated tissue (MALT) lymphomas (Supplementary Table 1). Three Hodgkin's-lymphoma-derived cell lines were also analysed. Interrogating more than 250,000 SNP sites, this platform permitted the identification of copy number changes at an average resolution of less than 12 kilobases (kb). The use of large numbers of

SNP-specific probes is a unique feature of this platform, and combined with the CNAG/AsCNAR software, enabled accurate determination of 'allele-specific' copy numbers, and thus allowed for sensitive detection of loss of heterozygosity (LOH) even without apparent copy-number reduction, in the presence of up to 70–80% normal cell contamination^{12,13}.

Lymphoma genomes underwent a wide range of genetic changes, including numerical chromosomal abnormalities and segmental gains and losses of chromosomal material (Supplementary Fig. 1), as well as copy-number-neutral LOH, or uniparental disomy (Supplementary Fig. 2). Each histology type had a unique genomic signature, indicating a distinctive underlying molecular pathogenesis for different histology types (Fig. 1a and Supplementary Fig. 3). On the basis of the genomic signatures, the initial pathological diagnosis of MCL was re-evaluated and corrected to DLBCL in two cases. Although most copy number changes involved large chromosomal segments, a number of regions showed focal gains and deletions, accelerating identification of their candidate gene targets. After excluding known copy number variations, we identified 46 loci showing focal gains (19 loci) or deletions (27 loci) (Supplementary Tables 2 and 3 and Supplementary Fig. 4).

Genetic lesions on the NF- κ B pathway were common in B-cell lymphomas and found in approximately 40% of the cases (Supplementary Table 1), underpinning the importance of aberrant NF- κ B activation in lymphomagenesis^{11,14} in a genome-wide fashion. They included focal gain/amplification at the *REL* locus (16.4%) (Fig. 1b) and *TRAF6* locus (5.9%), as well as focal deletions at the *PTEN* locus (5.5%) (Supplementary Figs 1 and 4). However, the most striking finding was the common deletion at 6q23.3 involving a 143-kb segment. It exclusively contained the *A20* gene (also called *TNFAIP3*), a negative regulator of NF- κ B activation^{2-7,15} (Fig. 1b), which was previously reported as a candidate target of 6q23 deletions in ocular lymphoma¹⁶. LOH involving the *A20* locus was found in 50 cases, of which 12 showed homozygous deletions as determined by the loss of both alleles in an allele-specific copy number analysis (Fig. 1b, Table 1 and Supplementary Table 4). On the basis of this finding, we searched for possible tumour-specific mutations of A20 by genomic DNA sequencing of entire coding exons of the gene in the same series of lymphoma samples (Supplementary Fig. 5). Because two out of the three Hodgkin's-lymphoma-derived cell lines had biallelic A20 deletions/mutations (Supplementary Fig. 6), 24 primary samples from Hodgkin's lymphoma were also analysed for mutations, where

¹Cancer Genomics Project, Department of ²Pediatrics, ³Cell Therapy and Transplantation Medicine, and ⁴Hematology and Oncology, Graduate School of Medicine, University of Tokyo, 7-3-1 Hongo, Bunkyo-ku, Tokyo 113-8655, Japan. ⁵Core Research for Evolutional Science and Technology, Japan Science and Technology Agency, 4-1-8, Honcho, Kawaguchi-shi, Saitama 332-0012, Japan. ⁶Department of Pediatrics, Graduate School of Medicine, Kyoto University, 54 Kawahara-cho, Shogoin, Sakyo-ku, Kyoto 606-8507, Japan. ⁷Department of Pathology, Okayama University Graduate School of Medicine, Dentistry and Pharmaceutical Sciences, 2-5-1 Shikata-cho, Kita-ku, Okayama 700-8558, Japan. ⁸Division of Pathology, The Cancer Institute of Japanese Foundation for Cancer Research, Japan, 3-10-6 Ariake, Koto-ku, Tokyo 135-8550, Japan. ⁹Hematology Division, Hospital, and ¹⁰Early Oncogenesis Research Project, Research Institute, National Cancer Center, 5-1-1 Tsukiji, Chuo-ku, Tokyo 104-0045, Japan. ¹¹Division of Immunology, Aichi Cancer Center Research Institute, 1-1 Kanokoden, Chikusa-ku, Nagoya 464-8681, Japan. ¹²Gunma Children's Medical Center, 779 Shimohakoda, Hokkitsu-machi, Shibukawa 377-8577, Japan. ¹³Division of Hematology, Internal Medicine, Showa University Fujigaoka Hospital, 1-30, Fujigaoka, Aoba-ku, Yokohama-shi, Kanagawa 227-8501, Japan. ¹⁴Department of Pathology, Teikyo University School of Medicine, 2-11-1 Kaga, Itabashi-ku, Tokyo 173-8605, Japan.

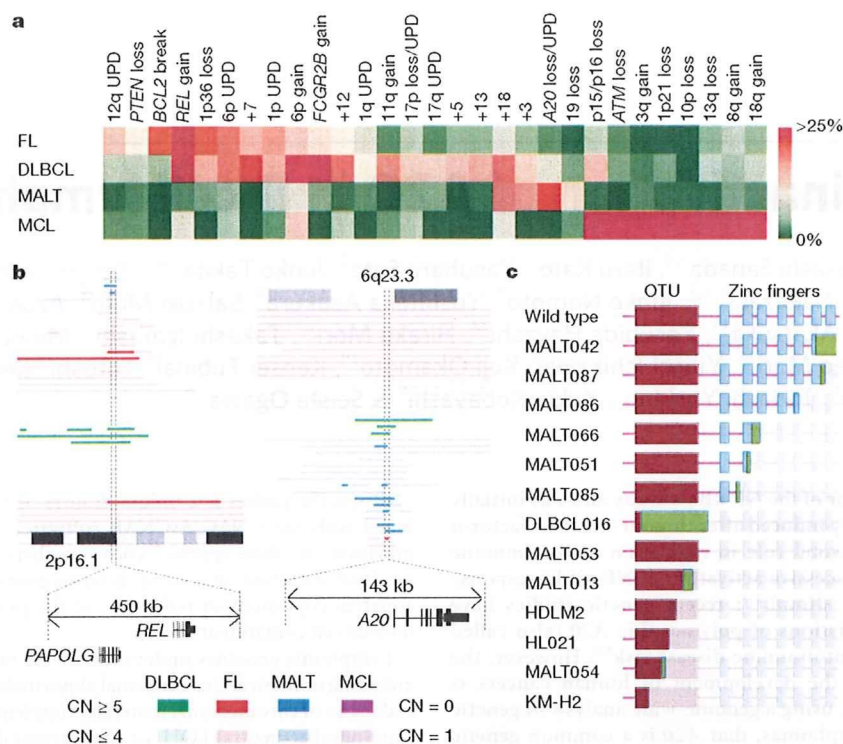


Figure 1 | Genomic signatures of different B-cell lymphomas and common genetic lesions at 2p16-15 and 6q23.3 involving NF- κ B pathway genes.

a, Twenty-nine genetic lesions were found in more than 10% in at least one histology and used for clustering four distinct histology types of B-lineage lymphomas. The frequency of each genetic lesion in each histology type is colour-coded. FL, follicular lymphoma; UPD, uniparental disomy.

b, Recurrent genetic changes are depicted based on CNAG output of the SNP array analysis of 238 B-lineage lymphoma samples, which include gains at the *REL* locus on 2p16-15 (left panel) and the *A20* locus on 6q23.3 (right

panel). Regions showing copy number gain or loss are indicated by horizontal lines. Four histology types are indicated by different colours, where high-grade amplifications and homozygous deletions are shown by darker shades to discriminate from simple gains (copy number ≤ 4) and losses (copy number = 1) (lighter shades). **c**, Point mutations and small nucleotide insertions and deletions in the *A20* (*TNEAIP3*) gene caused premature truncation of *A20* in most cases. Altered amino acids caused by frame shifts are indicated by green bars.

genomic DNA was extracted from 150 microdissected CD30-positive tumour cells (Reed–Sternberg cells) for each sample. *A20* mutations were found in 18 out of 265 lymphoma samples (6.8%) (Table 1), among which 13 mutations, including nonsense mutations (3 cases), frame-shift insertions/deletions (9 cases), and a splicing donor site mutation (1 case) were thought to result in premature termination of translation (Fig. 1c). Four missense mutations and one intronic mutation were identified in five microdissected Hodgkin's lymphoma samples. They were not found in the surrounding normal tissues, and thus, were considered as tumour-specific somatic changes.

In total, biallelic *A20* lesions were found in 31 out of 265 lymphoma samples including 3 Hodgkin's lymphoma cell lines. Quantitative analysis of SNP array data suggested that these *A20* lesions were present in the major tumour fraction within the samples (Supplementary Fig. 7). Inactivation of *A20* was most frequent in MALT lymphoma (18 out of 87) and Hodgkin's lymphoma (7 out of 27), although it was also found in DLBCL (5 out of 64) and follicular lymphoma (1 out of 52) at lower frequencies. In MALT lymphoma, biallelic *A20* lesions were confirmed in 18 out of 24 cases (75.0%) with LOH involving the 6q23.3 segment (Supplementary Fig. 8). Considering the limitation in detecting very small homozygous deletions, *A20* was thought to be the target of 6q23 LOH in MALT lymphoma. On the other hand, the 6q23 LOHs in other histology types tended to be extended into more centromeric regions and less frequently accompanied biallelic *A20* lesions (Supplementary Fig. 8 and Supplementary Table 4), indicating that they might be more

heterogeneous with regard to their gene targets. We were unable to analyse Hodgkin's lymphoma samples using SNP arrays owing to insufficient genomic DNA obtained from microdissected samples, and were likely to underestimate the frequency of *A20* inactivation in Hodgkin's lymphoma because we might fail to detect a substantial proportion of cases with homozygous deletions, which explained 50% (12 out of 24) of *A20* inactivation in other histology types. *A20* mutations in Hodgkin's lymphoma were exclusively found in nodular sclerosis classical Hodgkin's lymphoma (5 out of 15) but not in other histology types (0 out of 9), although the possible association requires further confirmation in additional cases.

A20 is a key regulator of NF- κ B signalling, negatively modulating NF- κ B activation through a wide variety of cell surface receptors and viral proteins, including tumour-necrosis factor (TNF) receptors, toll-like receptors, CD40, as well as Epstein–Barr-virus-associated LMP1 protein^{2,5,17,18}. To investigate the role of *A20* inactivation in lymphomagenesis, we re-expressed wild-type *A20* under a *Tet*-inducible promoter in a lymphoma-derived cell line (KM-H2) that had no functional *A20* alleles (Supplementary Fig. 6), and examined the effect of *A20* re-expression on cell proliferation, survival and downstream NF- κ B signalling pathways. As shown in Fig. 2a–c and Supplementary Fig. 9, re-expression of wild-type *A20* resulted in the suppression of cell proliferation and enhanced apoptosis, and in the concomitant accumulation of I κ B β and I κ B ϵ , and downregulation of NF- κ B activity. In contrast, re-expression of two lymphoma-derived *A20* mutants, *A20*^{532Stop} or *A20*^{750Stop}, failed to show growth suppression, induction of apoptosis, accumulation of I κ B β and I κ B ϵ or downregulation of

Table 1 | Inactivation of A20 in B-lineage lymphomas

Histology	Tissue	Sample	Allele	Uniparental disomy	Exon	Mutation	Biallelic inactivation
DLBCL	Lymph node	DLBCL008	-/-	No	-	-	5 out of 64 (7.8%)
	Lymph node	DLBCL016	+/-	No	Ex2	329insA	
	Lymph node	DLBCL022	-/-	No	-	-	
	Lymph node	DLBCL028	-/-	Yes	-	-	
	Lymph node	MCL008*	-/-	Yes	-	-	
Follicular lymphoma	Lymph node	FL024	-/-	No	-	-	1 out of 52 (1.9%)
MCL							0 out of 35 (0%)
MALT							18 out of 87 (21.8%)
Stomach							3 out of 23 (13.0%)
	Gastric mucosa	MALT013	+/+	Yes	Ex5	705insG	
	Gastric mucosa	MALT014	+/+	Yes	Ex3	Ex3 donor site>A	
	Gastric mucosa	MALT036	+/-	No	Ex7	deletion6-Ex7†	
Eye	Ocular adnexa	MALT008	-/-	No	-	-	13 out of 43 (30.2%)
	Ocular adnexa	MALT017	-/-	No	-	-	
	Ocular adnexa	MALT051	+/-	No	Ex7	1943delTG	
	Ocular adnexa	MALT053	+/+	Yes	Ex6	1016G>A(stop)	
	Ocular adnexa	MALT054	+/-	No	Ex3	502delTC	
	Ocular adnexa	MALT055	-/-	No	-	-	
	Ocular adnexa	MALT066	+/-	No	Ex7	1581insA	
	Ocular adnexa	MALT067	-/-	No	-	-	
	Ocular adnexa	MALT082	-/-	Yes	-	-	
	Ocular adnexa	MALT084	-/-	Yes	-	-	
	Ocular adnexa	MALT085	+/+	Yes	Ex7	1435insG	
	Ocular adnexa	MALT086	+/+	Yes	Ex6	878C>T(stop)	
	Ocular adnexa	MALT087	+/+	Yes	Ex9	2304delGG	
Lung	Lung	MALT042	-/-	No	-	-	2 out of 12 (16.7%)
	Lung	MALT047	+/+	Yes	Ex9	2281insT	
Other‡							0 out of 9 (0%)
Hodgkin's lymphoma							7 out of 27 (26.0%)
NSHL	Lymph node	HL10	ND	ND	Ex7	1777G>A(V571I)	
NSHL	Lymph node	HL12	ND	ND	Ex7	1156A>G(R364G)	
NSHL	Lymph node	HL21	ND	ND	Ex4	569G>A(stop)	
NSHL	Lymph node	HL24	ND	ND	Ex3	1487C>A(T474N)	
NSHL	Lymph node	HL23	ND	ND	-	Intron 3§	
	Cell line	KM-H2	-/-	No	-	-	
	Cell line	H2LM2	+/-	No	Ex4	616ins29bp	
Total							31 out of 265 (11.7%)

DLBCL, diffuse large B-cell lymphoma; MALT, MALT lymphoma; MCL, mantle cell lymphoma; ND, not determined because SNP array analysis was not performed; NSHL, nodular sclerosis classical Hodgkin's lymphoma.

*Diagnosis was changed based on the genomic data, which was confirmed by re-examination of pathology.

†Deletion including the boundary of intron 6 and exon 7 (see also Supplementary Fig. 5b).

‡Including 1 parotid gland, 1 salivary gland, 2 colon and 5 thyroid cases.

§Insertion of CTC at -19 bases from the beginning of exon 3.

||Insertion of TGGCTCCACAGACACACCCATGGCCCGA.

NF- κ B activity (Fig. 2a–c), indicating that these were actually loss-of-function mutations. To investigate the role of A20 inactivation in lymphomagenesis *in vivo*, A20- and mock-transduced KM-H2 cells were transplanted in NOD/SCID/ γ c^{null} (NOG) mice¹⁹, and their tumour formation status was examined for 5 weeks with or without induction of wild-type A20 by tetracycline administration. As shown in Fig. 2d, mock-transduced cells developed tumours at the injected sites, whereas the Tet-inducible A20-transduced cells generated tumours only in the absence of A20 induction (Supplementary Table 5), further supporting the tumour suppressor role of A20 in lymphoma development.

Given the mode of negative regulation of NF- κ B signalling, we next investigated the origins of NF- κ B activity that was deregulated by A20 loss in KM-H2 cells. The conditioned medium prepared from a 48-h serum-free KM-H2 culture had increased NF- κ B upregulatory activity compared with fresh serum-free medium, which was inhibited by re-expression of A20 (Fig. 3a). KM-H2 cells secreted two known ligands for TNF receptor—TNF- α and lymphotoxin- α (Supplementary Fig. 10)²⁰—and adding neutralizing antibodies against these cytokines into cultures significantly suppressed their cell growth and NF- κ B activity without affecting the levels of their overall suppression after A20

induction (Fig. 3b, d). In addition, recombinant TNF- α and/or lymphotoxin- α added to fresh serum-free medium promoted cell growth and NF- κ B activation in KM-H2 culture, which were again suppressed by re-expression of A20 (Fig. 3c, e). Although our data in Fig. 3 also show the presence of factors other than TNF- α and lymphotoxin- α in the KM-H2-conditioned medium—as well as some intrinsic pathways in the cell (Fig. 3a)—that were responsible for the A20-dependent NF- κ B activation, these results indicate that both cell growth and NF- κ B activity that were upregulated by A20 inactivation depend at least partly on the upstream stimuli that evoked the NF- κ B-activating signals.

Aberrant activation of the NF- κ B pathway is a hallmark of several subtypes of B-lineage lymphomas, including Hodgkin's lymphoma, MALT lymphoma, and a subset of DLBCL, as well as other lymphoid neoplasms^{11,14}, where a number of genetic alterations of NF- κ B signalling pathway genes^{21–25}, as well as some viral proteins^{26,27}, have been implicated in the aberrant activation of the NF- κ B pathway¹⁴. Thus, frequent inactivation of A20 in Hodgkin's lymphoma and MALT and other lymphomas provides a novel insight into the molecular pathogenesis of these subtypes of B-lineage lymphomas through deregulated NF- κ B activation. Because A20 provides a

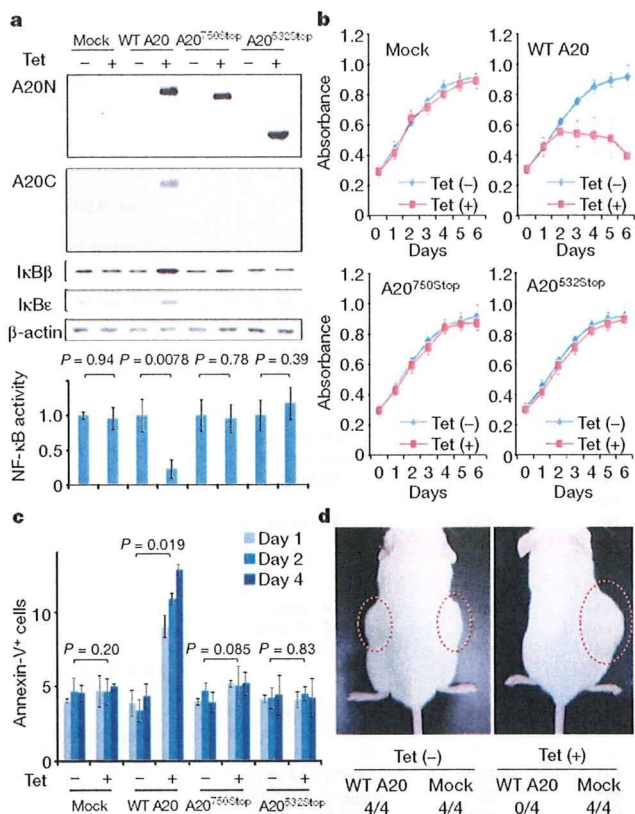


Figure 2 | Effects of wild-type and mutant A20 re-expressed in a lymphoma cell line that lacks the normal A20 gene. **a**, Western blot analyses of wild-type (WT) and mutant (A20^{532Stop} and A20^{750Stop}) A20, as well as IκBβ and IκBε, in KM-H2 cells, in the presence or absence of tetracycline treatment (top panels). A20N and A20C are polyclonal antisera raised against N-terminal and C-terminal A20 peptides, respectively. β-actin blots are provided as a control. NF-κB activities are expressed as mean absorbance ± s.d. (*n* = 6) in luciferase assays (bottom panel). **b**, Proliferation of KM-H2 cells stably transfected with plasmids for mock and Tet-inducible wild-type A20, A20^{532Stop} and A20^{750Stop} was measured using a cell counting kit in the presence (red lines) or absence (blue lines) of tetracycline. Mean absorbance ± s.d. (*n* = 5) is plotted. **c**, The fractions of Annexin-V-positive KM-H2 cells transfected with various Tet-inducible A20 constructs were measured by flow cytometry after tetracycline treatment and the mean values (±s.d., *n* = 3) are plotted. **d**, *In vivo* tumorigenicity was assayed by inoculating 7×10^6 KM-H2 cells transfected with mock or Tet-inducible wild-type A20 in NOG mice, with (right panel) or without (left panel) tetracycline administration.

negative feedback mechanism in the regulation of NF-κB signalling pathways upon a variety of stimuli, aberrant activation of NF-κB will be a logical consequence of A20 inactivation. However, there is also the possibility that the aberrant NF-κB activity of A20-inactivated lymphoma cells is derived from upstream stimuli, which may be from the cellular environment. In this context, it is intriguing that MALT lymphoma usually arises at the site of chronic inflammation caused by infection or autoimmune disorders and may show spontaneous regression after eradication of infectious organisms³⁸; furthermore, Hodgkin's lymphoma frequently shows deregulated cytokine production from Reed–Sternberg cells and/or surrounding reactive cells²⁹. Detailed characterization of the NF-κB pathway regulated by A20 in both normal and neoplastic B lymphocytes will promote our understanding of the precise roles of A20 inactivation in the pathogenesis of these lymphoma types. Our finding underscores the importance of genome-wide approaches in the identification of genetic targets in human cancers.

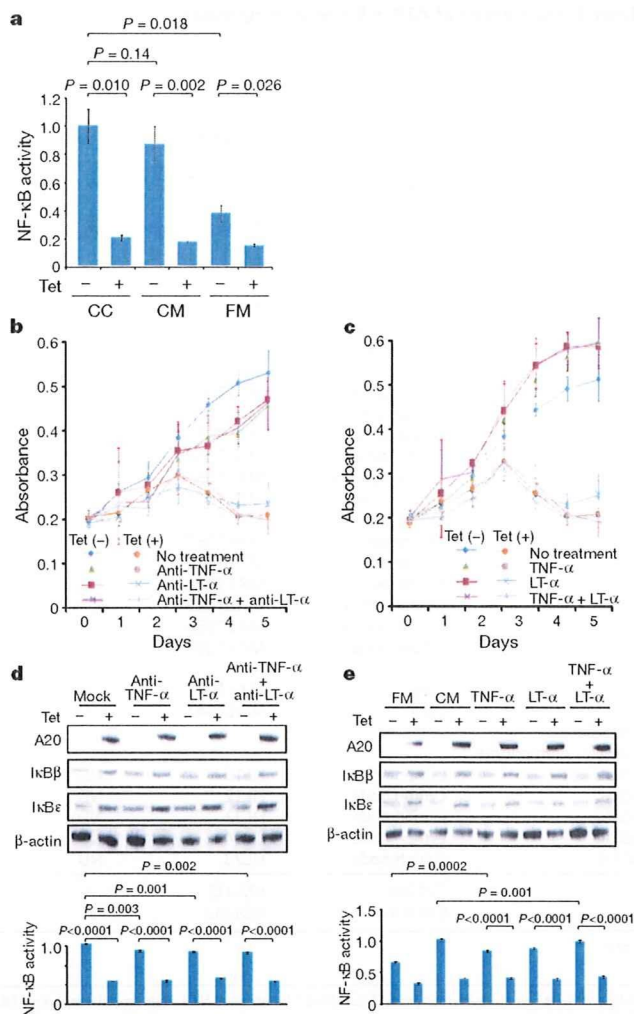


Figure 3 | Tumour suppressor role of A20 under external stimuli. **a**, NF-κB activity in KM-H2 cells was measured 30 min after cells were inoculated into fresh medium (FM) or KM-H2-conditioned medium (CM) obtained from the 48-h culture of KM-H2, and was compared with the activity after 48 h continuous culture of KM-H2 (CC). A20 was induced 12 h before inoculation in Tet (+) groups. **b**, **c**, Effects of neutralizing antibodies against TNF-α and lymphotoxin-α (LT-α) (**b**) and of recombinant TNF-α and LT-α added to the culture (**c**) on cell growth were evaluated in the presence (Tet (+)) or absence (Tet (-)) of A20 induction. Cell numbers were measured using a cell counting kit and are plotted as their mean absorbance ± s.d. (*n* = 6). **d**, **e**, Effects of the neutralizing antibodies (**d**) and the recombinant cytokines added to the culture (**e**) on NF-κB activities and the levels of IκBβ and IκBε after 48 h culture with (Tet (+)) or without (Tet (-)) tetracycline treatment. NF-κB activities are expressed as mean absorbance ± s.d. (*n* = 6) in luciferase assays.

METHODS SUMMARY

Genomic DNA from 238 patients with non-Hodgkin's lymphoma and three Hodgkin's-lymphoma-derived cell lines was analysed using GeneChip SNP genotyping microarrays (Affymetrix). This study was approved by the ethics boards of the University of Tokyo, National Cancer Institute Hospital, Okayama University, and the Cancer Institute of the Japanese Foundation of Cancer Research. After appropriate normalization of mean array intensities, signal ratios between tumours and anonymous normal references were calculated in an allele-specific manner, and allele-specific copy numbers were inferred from the observed signal ratios based on the hidden Markov model using CNAG/AsCNAR software (<http://www.genome.umin.jp>). A20 mutations were examined by directly sequencing genomic DNA using a set of primers (Supplementary Table 6). Full-length cDNAs of wild-type and mutant A20 were introduced into a

lentivirus vector, pLenti4/TO/V5-DEST (Invitrogen), with a *Tet*-inducible promoter. Viral stocks were prepared by transfecting the vector plasmids into 293FT cells (Invitrogen) using the calcium phosphate method and then infected to the KM-H2 cell line. Proliferation of KM-H2 cells was measured using a Cell Counting Kit (Dojindo). Western blot analyses and luciferase assays were performed as previously described. NF- κ B activity was measured by luciferase assays in KM-H2 cells stably transduced with a reporter plasmid having an NF- κ B response element, pGL4.32 (Promega). Apoptosis of KM-H2 upon A20 induction was evaluated by counting Annexin-V-positive cells by flow cytometry. For *in vivo* tumorigenicity assays, 7×10^6 KM-H2 cells were transduced with the *Tet*-inducible A20 gene and those with a mock vector were inoculated on the contralateral sides in eight NOG mice¹⁹ and examined for their tumour formation with ($n = 4$) or without ($n = 4$) tetracycline administration. Full copy number data of the 238 lymphoma samples will be accessible from the Gene Expression Omnibus (GEO, <http://ncbi.nlm.nih.gov/geo/>) with the accession number GSE12906.

Full Methods and any associated references are available in the online version of the paper at www.nature.com/nature.

Received 17 September 2008; accepted 3 March 2009.

Published online 3 May 2009.

- Dixit, V. M. *et al.* Tumor necrosis factor- α induction of novel gene products in human endothelial cells including a macrophage-specific chemotaxin. *J. Biol. Chem.* **265**, 2973–2978 (1990).
- Song, H. Y., Rothe, M. & Goeddel, D. V. The tumor necrosis factor-inducible zinc finger protein A20 interacts with TRAF1/TRAF2 and inhibits NF- κ B activation. *Proc. Natl Acad. Sci. USA* **93**, 6721–6725 (1996).
- Lee, E. G. *et al.* Failure to regulate TNF-induced NF- κ B and cell death responses in A20-deficient mice. *Science* **289**, 2350–2354 (2000).
- Boone, D. L. *et al.* The ubiquitin-modifying enzyme A20 is required for termination of Toll-like receptor responses. *Nature Immunol.* **5**, 1052–1060 (2004).
- Wang, Y. Y., Li, L., Han, K. J., Zhai, Z. & Shu, H. B. A20 is a potent inhibitor of TLR3- and Sendai virus-induced activation of NF- κ B and ISRE and IFN- β promoter. *FEBS Lett.* **576**, 86–90 (2004).
- Wertz, I. E. *et al.* De-ubiquitination and ubiquitin ligase domains of A20 downregulate NF- κ B signalling. *Nature* **430**, 694–699 (2004).
- Heynck, K. & Beyaert, R. A20 inhibits NF- κ B activation by dual ubiquitin-editing functions. *Trends Biochem. Sci.* **30**, 1–4 (2005).
- Graham, R. R. *et al.* Genetic variants near *TNFAIP3* on 6q23 are associated with systemic lupus erythematosus. *Nature Genet.* **40**, 1059–1061 (2008).
- Musone, S. L. *et al.* Multiple polymorphisms in the *TNFAIP3* region are independently associated with systemic lupus erythematosus. *Nature Genet.* **40**, 1062–1064 (2008).
- Jaffe, E. S., Harris, N. L., Stein, H. & Vardiman, J. W. *World Health Organization Classification of Tumours. Pathology and Genetics of Tumours of Hematopoietic and Lymphoid Tissues* (IARC Press, 2001).
- Klein, U. & Dalla-Favera, R. Germinal centres: role in B-cell physiology and malignancy. *Nature Rev. Immunol.* **8**, 22–33 (2008).
- Nannya, Y. *et al.* A robust algorithm for copy number detection using high-density oligonucleotide single nucleotide polymorphism genotyping arrays. *Cancer Res.* **65**, 6071–6079 (2005).
- Yamamoto, G. *et al.* Highly sensitive method for genomewide detection of allelic composition in nonpaired, primary tumor specimens by use of affymetrix single-nucleotide-polymorphism genotyping microarrays. *Am. J. Hum. Genet.* **81**, 114–126 (2007).
- Jost, P. J. & Ruland, J. Aberrant NF- κ B signaling in lymphoma: mechanisms, consequences, and therapeutic implications. *Blood* **109**, 2700–2707 (2007).
- Durkop, H., Hirsch, B., Hahn, C., Foss, H. D. & Stein, H. Differential expression and function of A20 and TRAF1 in Hodgkin lymphoma and anaplastic large cell lymphoma and their induction by CD30 stimulation. *J. Pathol.* **200**, 229–239 (2003).
- Honma, K. *et al.* *TNFAIP3* is the target gene of chromosome band 6q23.3-q24.1 loss in ocular adnexal marginal zone B cell lymphoma. *Genes Chromosom. Cancer* **47**, 1–7 (2008).
- Sarma, V. *et al.* Activation of the B-cell surface receptor CD40 induces A20, a novel zinc finger protein that inhibits apoptosis. *J. Biol. Chem.* **270**, 12343–12346 (1995).
- Fries, K. L., Miller, W. E. & Raab-Traub, N. The A20 protein interacts with the Epstein-Barr virus latent membrane protein 1 (LMP1) and alters the LMP1/TRAF1/TRADD complex. *Virology* **264**, 159–166 (1999).
- Hiramatsu, H. *et al.* Complete reconstitution of human lymphocytes from cord blood CD34⁺ cells using the NOD/SCID/ γ^c mice model. *Blood* **102**, 873–880 (2003).
- Hsu, P. L. & Hsu, S. M. Production of tumor necrosis factor- α and lymphotoxin by cells of Hodgkin's neoplastic cell lines HDLM-1 and KM-H2. *Am. J. Pathol.* **135**, 735–745 (1989).
- Dierlamm, J. *et al.* The apoptosis inhibitor gene *API2* and a novel 18q gene, *MLT1*, are recurrently rearranged in the t(11;18)(q21;q21) associated with mucosa-associated lymphoid tissue lymphomas. *Blood* **93**, 3601–3609 (1999).
- Willis, T. G. *et al.* Bcl10 is involved in t(1;14)(p22;q32) of MALT B cell lymphoma and mutated in multiple tumor types. *Cell* **96**, 35–45 (1999).
- Joos, S. *et al.* Classical Hodgkin lymphoma is characterized by recurrent copy number gains of the short arm of chromosome 2. *Blood* **99**, 1381–1387 (2002).
- Martin-Subero, J. I. *et al.* Recurrent involvement of the *REL* and *BCL11A* loci in classical Hodgkin lymphoma. *Blood* **99**, 1474–1477 (2002).
- Lenz, G. *et al.* Oncogenic *CARD11* mutations in human diffuse large B cell lymphoma. *Science* **319**, 1676–1679 (2008).
- Deacon, E. M. *et al.* Epstein-Barr virus and Hodgkin's disease: transcriptional analysis of virus latency in the malignant cells. *J. Exp. Med.* **177**, 339–349 (1993).
- Yin, M. J. *et al.* HTLV-1 Tax protein binds to MEK1 to stimulate I κ B kinase activity and NF- κ B activation. *Cell* **93**, 875–884 (1998).
- Isaacson, P. G. & Du, M. Q. MALT lymphoma: from morphology to molecules. *Nature Rev. Cancer* **4**, 644–653 (2004).
- Skinider, B. F. & Mak, T. W. The role of cytokines in classical Hodgkin lymphoma. *Blood* **99**, 4283–4297 (2002).

Supplementary Information is linked to the online version of the paper at www.nature.com/nature.

Acknowledgements This work was supported by the Core Research for Evolutional Science and Technology, Japan Science and Technology Agency, by the 21st century centre of excellence program 'Study on diseases caused by environment/genome interactions', and by Grant-in-Aids from the Ministry of Education, Culture, Sports, Science and Technology of Japan and from the Ministry of Health, Labor and Welfare of Japan for the 3rd-term Comprehensive 10-year Strategy for Cancer Control. We also thank Y. Ogino, E. Matsui and M. Matsumura for their technical assistance.

Author Contributions M.Ka., K.N. and M.S. performed microarray experiments and subsequent data analyses. M.Ka., Y.C., K.Ta., J.T., J.N., M.I., A.T. and Y.K. performed mutation analysis of A20. M.Ka., S.Mu., M.S., Y.C. and Y.Ak. conducted functional assays of mutant A20. Y.S., K.Ta., Y.As., H.M., M.Ku., S.Mo., S.C., Y.K., K.To. and Y.I. prepared tumour specimens. I.K., K.O., A.N., H.N. and T.N. conducted *in vivo* tumorigenicity experiments in NOG/SCID mice. T.I., Y.H., T.Y., Y.K. and S.O. designed overall studies, and S.O. wrote the manuscript. All authors discussed the results and commented on the manuscript.

Author Information The copy number data as well as the raw microarray data will be accessible from the GEO (<http://ncbi.nlm.nih.gov/geo/>) with the accession number GSE12906. Reprints and permissions information is available at www.nature.com/reprints. Correspondence and requests for materials should be addressed to S.O. (sogawa-ky@umin.ac.jp) or Y.K. (ykkobaya@ncc.go.jp).

METHODS

Specimens. Primary tumour specimens were obtained from patients who were diagnosed with DLBCL, follicular lymphoma, MCL, MALT lymphoma, or classical Hodgkin's lymphoma. In total, 238 primary lymphoma specimens listed in Supplementary Table 1 were subjected to SNP array analysis. Three Hodgkin's lymphoma-derived cell lines (KM-H2, HDLM2, L540) were obtained from Hayashibara Biochemical Laboratories, Inc., Fujisaki Cell Center and were also analysed by SNP array analysis.

Microarray analysis. High-molecular-mass DNA was isolated from tumour specimens and subjected to SNP array analysis using GeneChip Mapping 50K and/or 250K arrays (Affymetrix). The scanned array images were processed with Gene Chip Operation software (GCOS), followed by SNP calls using GTYPE. Genome-wide copy number measurements and LOH detection were performed using CNAG/AsCNAR software^{12,13}.

Mutation analysis. Mutations in the *A20* gene were examined in 265 samples of B-lineage lymphoma, including 62 DLBCLs, 52 follicular lymphomas, 87 MALTs, 37 MCLs and 3 Hodgkin's lymphoma-derived cell lines and 24 primary Hodgkin's lymphoma samples, by direct sequencing using an ABI PRISM 3130xl Genetic Analyser (Applied Biosystems). To analyse primary Hodgkin's lymphoma samples in which CD30-positive tumour cells (Reed–Sternberg cells) account for only a fraction of the specimen, 150 Reed–Sternberg cells were collected for each 10 μ m slice of a formalin-fixed block immunostained for CD30 by laser-capture microdissection (ASLMD6000, Leica), followed by genomic DNA extraction using QIAamp DNA Micro kit (Qiagen). The primer sets used in this study are listed in Supplementary Table 6.

Functional analysis of wild-type and mutant *A20*. Full-length cDNA for wild-type *A20* was isolated from total RNA extracted from an acute myeloid leukaemia-derived cell line, CTS, and subcloned into a lentivirus vector (pLenti4/TO/V5-DEST, Invitrogen). cDNAs for mutant *A20* were generated by PCR amplification using mutagenic primers (Supplementary Table 6), and introduced into the same lentivirus vector. Forty-eight hours after transfection of each plasmid into 293FT cells using the calcium phosphate method, lentivirus stocks were obtained from ultrafiltration using Amicon Ultra (Millipore), and used to infect KM-H2 cells to generate stable transfectants of mock, wild-type and mutant *A20*. Each KM-H2 derivative cell line was further transduced stably with a reporter plasmid (pGL4.32, Promega) containing a luciferase gene under an NF- κ B-responsive element by electroporation using Nucleofector reagents (Amaxa).

Assays for cell proliferation and NF- κ B activity. Proliferation of the KM-H2 derivative cell lines was assayed in triplicate using a Cell Counting Kit (Dojindo). The mean absorption of five independent assays was plotted with s.d. for each derivative line. Two independent KM-H2-derived cell lines were used for each experiment. The NF- κ B activity in KM-H2 derivatives for *A20* mutants was evaluated by luciferase assays using a PiccaGene Luciferase Assay Kit (TOYO B-Net Co.). Each assay was performed in triplicate and the mean absorption of five independent experiments was plotted with s.d.

Western blot analyses. Polyclonal anti-sera against N-terminal (anti-A20N) and C-terminal (anti-A20C) *A20* peptides were generated by immunizing rabbits with

these peptides (LSNMRKAVKIRERTPEDIC for anti-A20N and CFQFKQMYG for anti-A20C, respectively). Total cell lysates from KM-H2 cells were separated on 7.5% polyacrylamide gel and subjected to western blot analysis using antibodies to *A20* (anti-A20N and anti-A20C), I κ B α (sc-847), I κ B β (sc-945), I κ B γ (sc-7155) and actin (sc-8432) (Santa Cruz Biotechnology).

Functional analyses of wild-type and mutant *A20*. Each KM-H2 derivative cell line stably transduced with various *Tet*-inducible *A20* constructs was cultured in serum-free medium in the presence or absence of *A20* induction using 1 μ g ml⁻¹ of tetracycline, and cell number was counted every day. 1 \times 10⁶ cells of each KM-H2 derivative cell line were analysed for their intracellular levels of I κ B β and I κ B ϵ and for NF- κ B activities by western blot analyses and luciferase assays, respectively, 12 h after the beginning of cell culture. Effects of human recombinant TNF- α and lymphotoxin- α (210-TA and 211-TB, respectively, R&D Systems) on the NF- κ B pathway and cell proliferation were evaluated by adding both cytokines into 10 ml of serum-free cell culture at a concentration of 200 pg ml⁻¹. For cell proliferation assays, culture medium was half replaced every 12 h to minimize the side-effects of autocrine cytokines. Intracellular levels of I κ B β , I κ B ϵ and NF- κ B were examined 12 h after the beginning of the cell culture. To evaluate the effect of neutralizing TNF- α and lymphotoxin- α , 1 \times 10⁶ of KM-H2 cells transduced with both *Tet*-inducible *A20* and the NF- κ B-luciferase reporter were pre-cultured in serum-free media for 36 h, and thereafter neutralizing antibodies against TNF- α (MAB210, R&D Systems) and/or lymphotoxin- α (AF-211-NA, R&D Systems) were added to the media at a concentration of 200 pg ml⁻¹. After the extended culture during 12 h with or without 1 μ g ml⁻¹ tetracycline, the intracellular levels of I κ B β and I κ B ϵ and NF- κ B activities were examined by western blot analysis and luciferase assays, respectively. To examine the effects of *A20* re-expression on apoptosis, 1 \times 10⁶ KM-H2 cells were cultured for 4 days in 10 ml medium with or without *Tet* induction. After staining with phycoerythrin-conjugated anti-Annexin-V (ID556422, Becton Dickinson), Annexin-V-positive cells were counted by flow cytometry at the indicated times.

In vivo tumorigenicity assays. KM-H2 cells transduced with a mock or *Tet*-inducible wild-type *A20* gene were inoculated into NOG mice and their tumorigenicity was examined for 5 weeks with or without tetracycline administration. Injections of 7 \times 10⁶ cells of each KM-H2 cell line were administered to two opposite sites in four mice. Tetracycline was administered in drinking water at a concentration of 200 μ g ml⁻¹.

ELISA. Concentrations of TNF- α , lymphotoxin- α , IL-1, IL-2, IL-4, IL-6, IL-12, IL-18 and TGF- β in the culture medium were measured after 48 h using ELISA. For those cytokines detectable after 48-h culture (TNF α , LT α , and IL-6), their time course was examined further using the Quantikine ELISA kit (R&D Systems).

Statistical analysis. Significance of the difference in NF- κ B activity between two given groups was evaluated using a paired *t*-test, in which the data from each independent luciferase assay were paired to calculate test statistics. To evaluate the effect of *A20* re-expression in KM-H2 cells on apoptosis, the difference in the fractions of Annexin-V-positive cells between *Tet* (+) and *Tet* (-) groups was also tested by a paired *t*-test for assays, in which the data from the assays performed on the same day were paired.



Short communication

***NUP98–NSD3* fusion gene in radiation-associated myelodysplastic syndrome with t(8;11)(p11;p15) and expression pattern of NSD family genes**Takeshi Taketani^a, Tomohiko Taki^b, Hideo Nakamura^c, Masafumi Taniwaki^d, Junichi Masuda^a, Yasuhide Hayashi^{e,*}^aDivision of Blood Transfusion, Shimane University Hospital, Izumo, Shimane, Japan^bDepartment of Molecular Laboratory Medicine, Kyoto Prefectural University of Medicine Graduate School of Medical Science, Kyoto, Japan^cDepartment of Internal Medicine, Koufudai Hospital, Nagasaki, Japan^dDepartment of Molecular Hematology and Oncology, Kyoto Prefectural University of Medicine Graduate School of Medical Science, Kyoto, Japan^eDepartment of Hematology/Oncology, Gunma Children's Medical Center, 779 Shimohakoda, Hokkitsu, Shibukawa, Gunma 377-8577, Japan

Received 9 September 2008; received in revised form 27 November 2008; accepted 15 December 2008

Abstract

Chromosomal 11p15 abnormality of therapy-related myelodysplastic syndrome (t-MDS)—acute myeloid leukemia (AML) is rare. *NUP98–NSD3* fusion transcripts have been detected previously in one patient with AML and one patient with t-MDS having t(8;11)(p11;p15). Here we present the case of a 60-year-old man with radiation-associated MDS (r-MDS) carrying chromosome abnormalities, including t(8;11)(p11;p15) and del(1)(p22p32). Fluorescence in situ hybridization analysis demonstrated that the *NUP98* gene at 11p15 was split by the translocation. Southern blot analysis of bone marrow cells showed both rearrangements of *NUP98* and *NSD3* genes. Reverse transcriptase–polymerase chain reaction (RT-PCR) followed by sequence analysis revealed the presence of both *NUP98–NSD3* and *NSD3–NUP98* fusion transcripts. Expression analysis by RT-PCR showed that *NSD3* as well as *NSD1* and *NSD2* was ubiquitously expressed in leukemic cell lines and Epstein–Barr virus transformed B lymphocyte cell lines derived from the normal adult lymphocytes examined. Two isoforms of *NSD3*, *NSD3S* and *NSD3L* (but not *NSD3L2*), were expressed in leukemic cell lines and were fused to *NUP98* in our patient, suggesting that qualitative change of these two isoforms of *NSD3* by fusion with *NUP98* might be related to leukemogenesis, although the function of each isoform of the *NSD3* gene remains unclear. © 2009 Elsevier Inc. All rights reserved.

1. Introduction

Myeloid malignancies with 11p15 translocations are likely to be related to the nucleoporin gene, *NUP98* [1]. These translocations produced fusion genes between *NUP98* and many different partner genes [1]. Four patients with t(8;11)(p11;p15) have been reported previously [2–5], and the four diagnosed with acute myeloid leukemia (AML) or therapy-related myelodysplastic syndrome (t-MDS). The *NUP98–NSD3* fusion gene was identified in only two of these four patients with t(8;11) [4,5].

Therapy-related myelodysplastic syndrome (t-MDS) is considered to be a heterogeneous disorder of pluripotent hematopoietic stem cells that have various findings of bone

marrow (BM) failure, often evolve to AML, and have a poor prognosis [6,7]. Although the pathogenesis of t-MDS is unknown, many recurrent chromosomal abnormalities are involved in t-MDS [8,9]. Only 17 patients were identified with 11p15 chromosomal abnormality among 511 patients with t-MDS–AML [10]. In the survey of Japanese childhood t-MDS–AML, 5 of 81 children had 11p15 translocations involving *NUP98* rearrangements [11].

Here we describe the case of a 60-year-old patient with radiation-associated MDS (r-MDS) patient exhibiting translocation t(8;11) and a *NUP98–NSD3* fusion transcript. We also report the expression of NSD family genes *NSD1*, *NSD2*, and *NSD3* in several leukemia and normal Epstein–Barr virus transformed B lymphocyte (EBV-B) cell lines from healthy volunteers.

We note that in the international human gene nomenclature (<http://www.genenames.org>), *NSD1* is an approved gene symbol, but *NSD2* and *NSD3* are classified as aliases,

* Corresponding author. Tel.: +81-279-52-3551 ext. 2200; fax: +81-279-52-2045.

E-mail address: hayashiy-tyk@umin.ac.jp (Y. Hayashi).

for *WHSC1* and *WHSC1L1*, respectively. In the present report, however, for convenience of discussion we continue to use the *NSD* nomenclature for all three genes.

2. Case report

A 60-year-old man was admitted for assessment of anemia. He had been an atomic-bomb survivor in Nagasaki 44 years before. When he was 59 years old, he was diagnosed with sigmoid colon cancer and underwent operative resection. His father died of lung cancer. On examination, blood examination showed a white blood cell count of 6,250/ μ L with no leukemic blasts, a hemoglobin level of 11.1 g/dL, and a platelet count of 337,500/ μ L. The BM examination revealed a nuclear cell count of 127,500/ μ L with no leukemic blasts. He had megakaryocytes with multiseparated nuclei and mature neutrophils with pseudo-Pelger–Huet anomaly. Conventional chromosomal analysis demonstrated 46,XY,t(8;11)(p11;p15),del(1)(p22p32) in all 20 BM cells examined. He was diagnosed with refractory anemia (RA), but was not treated; he developed AML, 1 year after the diagnosis of RA. Cytogenetic findings in the AML were the same as in the RA. He died of progressive disease 23 months after diagnosis of RA, despite low-dose cytarabine.

2.1. Fluorescence in situ hybridization analysis

The fluorescence in situ hybridization (FISH) analysis of the patient's leukemic cells using bacterial artificial chromosome (BAC) clone PK505 was performed as described previously [12]. We mapped this BAC clone to leukemic cells together with a whole-chromosome painting probe for chromosome 11 (WCP11) (Coatome 11, digoxigenin-labeled; Oncor, Gaithersburg, MD).

2.2. Southern blot analysis

After obtaining informed consent from the patient, high molecular weight DNA was extracted from BM cells by proteinase K digestion and phenol–chloroform extraction [13]. Ten micrograms of DNA were digested with *Eco*RI and *Bgl*II restriction endonucleases, subjected to electrophoresis on 0.7% agarose gels, transferred to nylon membrane, and hybridized to cDNA probes³²P-labeled by the random hexamer method [13]. The probes were an 837-bp *NUP98* cDNA fragment (nucleotide nt 1213 to 2049; GenBank accession no. U41815) and a 512-bp *NSD3* cDNA fragment (nt 929 to 1440; GenBank accession no. AJ295990).

2.3. Reverse transcriptase-polymerase chain reaction and nucleotide sequencing

NUP98–NSD3 chimeric mRNA was detected by reverse transcriptase–polymerase chain reaction (RT-PCR) in

essentially the same manner as described previously [14]. Total RNA was extracted from the leukemia cells of the patient using the guanidine thiocyanate–phenol–chloroform method [14]. Total RNA (4 μ g) was reverse-transcribed to cDNA, using a cDNA synthesis kit (GE Healthcare Bio-Science, Piscataway, NJ) [14]. The PCR was performed with AmpliTaq Gold DNA polymerase (Applied Biosystems, Tokyo, Japan), using the reagents recommended by the manufacturer.

The primers used for detection of *NUP98–NSD3* fusion transcripts and the reciprocal fusion transcripts were *NUP98–S10* (5'-TGGGACTCTTACTGGGCTT-3') and *NSD3–R4* (5'-CTCTCTGGCTGGTTGCTAAA-3') for *NUP98–NSD3*, and *NSD3–S1* (5'-CAAGATCTGAAGAGCGCAAG-3') and *NUP98–R13* (5'-TAGGGTCTGACATCGGATTC-3') for *NSD3–NUP98*. The PCR amplification was performed with this mixture using a DNA thermal cycler (Applied Biosystems) under the following conditions: initial denaturation at 94°C for 9 minutes, 40 cycles at 96°C for 30 seconds, 55°C for 30 seconds, and 72°C for 1 minute, followed by a final elongation at 72°C for 7 minutes.

For detection of *NUP98–NSD3L*, *NUP98–NSD3L2*, and *NUP98–NSD3S* fusions, nested RT-PCR was performed. The primers for first RT-PCR were *NUP98–S10* and *NSD3L–R* (5'-ACCTGGGGTTGCAGATCTCT-3'), *NUP983L2–R* (5'-AATCTTCCACCTCTGGCAC-3'), *NSD3S–R* (5'-ACGGAGCTGCTACTGAATCT-3'), respectively. The primers for second RT-PCR were *NUP98–S11* (5'-CCTCTTGGTACAGGAGCCTT-3') and *NSD3–R4*. The PCR conditions were as described above. The PCR products were subcloned into pCR2.1 vector (Invitrogen, Carlsbad, CA) and were sequenced by the fluorometric method using the Big Dye terminator cycle sequencing kit (Applied Biosystems).

2.4. Expression of three isoforms of the *NSD3* gene and the *NSD1* and *NSD2* genes by RT-PCR in leukemic cell lines

To analyze the expression pattern of three isoforms of the *NSD3* gene (*NSD3L*, *NSD3L2*, and *NSD3S*) and the family genes *NSD1* and *NSD2* in leukemic cell lines, RT-PCR was performed. In all, 59 cell lines were examined, as follows [14]: 10 B-precursor ALL cell lines (NALM-6, NALM-24, NALM-26, UTP-2, THP-4, RS4;11, SCMC-L10, KOCL-33, KOCL-45, and KOCL-69), 9 B-ALL cell lines (BALM-1, BALM-13, BALM-14, BJAB, DAUDI, RAJI, RAMOS, BAL-KH, and NAMALVA), 9 T-ALL cell lines (RPMI-8402, MOLT-14, THP-6, PEER, H-SB2, HPB-ALL, L-SAK, L-SMY, and KCMC-T), 8 AML cell lines (YNH-1, ML-1, KASUMI-3, KG-1, inv-3, SN-1, NB4, and HEL), 6 acute monocytic leukemic cell lines (THP-1, IMS/M1, CTS, P31/FUJ, MOLM-13, and KOCL-48), 5 chronic myelogenous leukemia cell lines (MOLM-1, MOLM-7, TS9;22, SS9;22, and K-562), 2 acute